50-400/401 OL

I-Eddl.-1
6/15/84

Eddleman Ex. 1

UCD 472-502
DOE Research and Development Report
UC-48, Biomedical and Environmental Research

SIZE DEPENDENCE OF THE PHYSICAL AND CHEMICAL PROPERTIES OF FLY ASH

good information on fine particles: can stay in air missed by [illegible] & stay in lung longer

G.L. Fisher
and
D.F.S. Natusch

Radiobiology Laboratory

[illegible] concentration in smaller [illegible]

UCD 472 - 502

SIZE DEPENDENCE OF THE PHYSICAL AND CHEMICAL PROPERTIES OF COAL FLY ASH

G. L. FISHER

Radiobiology Laboratory
University of California
Davis, California 95616

D. F. S. NATUSCH

Department of Chemistry
Colorado State University
Fort Collins, Colorado 80523

Quote this source

Spring, 1979

This report reproduces a chapter in: Analytical Methods for Coal and Coal Products, Volume III (C. Karr, Jr., editor), Academic Press, pp. 489 - 541, 1979.

This research was supported by the US Department of Energy.

I. INTRODUCTION

In order to assess the environmental significance and potential health hazards associated with exposure to environmental pollutants, detailed studies of physical and chemical properties are required. It is these properties that determine the route and biological consequences of exposure. The aerodynamic behavior of aerosols released during coal combustion will determine the potential for atmospheric transport and subsequent human exposure. Large particles (>10 μm) escaping the power plant's control technology will fall out near the plant, which may ultimately result in general population exposure by ingestion of agricultural products or water. Thus, exposure of agricultural products by soil or foliar deposition or contamination of water sources in the environs of the power plant will reflect, for the most part, the chemical composition of the larger particles. Long-range transport and general population exposure will be associated with the more stable aerosols. These fine particles (<10 μm) are of special interest because they are less efficiently collected by existing control technologies, have a relatively long atmospheric residence time, and upon inhalation, are efficiently deposited and slowly removed from the pulmonary region of the respiratory tract.

In a review of particulate abatement technologies, Vandegrift et al. (1973) described collection efficiency as a function of particle size for a variety of control technologies including electrostatic precipitators, fabric filters, wet scrubbers, and cyclones. Average collection efficiencies for a medium-efficiency electrostatic precipitator (ESP) were 90, 70, and 35% for 1.0, 0.1, and 0.01 μm particles, respectively. Interestingly, the Venturi wet scrubber (VWS) was more efficient (99.5%) for 1.0 μm particles and less efficient (<1%) for 0.01 μm particles. A crossover in the ESP- and VWS-efficiency curves was observed at 0.35 μm.

Respiratory tract deposition of inhaled particles is determined by the physics and chemistry of aerosols, the anatomy of the respiratory tract, and the airflow patterns in the lung airways (Yeh et al., 1976). The most important physical factors affecting lung deposition of inhaled particles are the aerodynamic properties of the aerosol and the chemical reactivity in the airways. Lung deposition is generally described in terms of fractional particulate deposition by mass or number in the three major regions of the respiratory tract: the nasopharyngeal, tracheobronchial, and pulmonary regions (Task Group on Lung Dynamics, 1966). The nasopharyngeal region is composed of the nose and throat, extending to the larynx; the tracheobronchial region consists of the trachea and bronchial tree, including the terminal bronchioles; and the pulmonary region consists of the respiratory bronchioles and the alveolar structures. Particles greater than 10 μm are effectively collected in the nasopharyngeal region; tracheobronchial and pulmonary deposition generally increase with decreasing particle size. Fractional deposition in the pulmonary region ranges from 30 to 60% of the inhaled aerosol for particles ranging in size from 1.0 to 0.01 μm (Task Group on Lung Dynamics, 1966). Similarly, tracheobronchial deposition ranges from 5 to 30% for inhaled aerosols from 1.0 to 0.01 μm, respectively. Respiratory tract deposition profiles have been calculated for iron, lead, and benzo(a)pyrene in urban aerosols (Natusch and Wallace, 1974). The hygroscopicity or

reactivity of an aerosol in the airways may dramatically alter the particle size and the regional deposition. Parks et al. (1977) have shown that, upon inhalation, ammoni sulfate aerosols with initial aerodynamic diameters of 0.8 μm and 8% relative humidity may rapidly grow to 2.3 μm in the water vapor saturated atmosphere of the respiratory tract. The rapid growth of the aerosols resulted in deposition predominantly in the nasopharyngeal region and lower than expected deposition in the tracheobronchial and pulmonary regions.

The rate of clearance of deposited particulate matter from the respiratory tract will be determined, in part, by the chemical behavior in the lung's unique microenvironment in the vicinity of the particle. Hygroscopic particles deposited in the respiratory tract will be rapidly cleared by dissolution and subsequent passage into the bloodstream for ultimate exposure of internal organs. Less soluble particles deposited on the mucocilliary escalator of the tracheobronchial region and on the ciliated epithelium of the nasopharyngeal region will be rapidly cleared with half-times on the order of one day and a few minutes, respectively (Task Group on Lung Dynamics, 1966). Relatively insoluble particles deposited in the pulmonary region will be phagocytized by the pulmonary alveolar macrophages (PAM). These particles will be slowly removed by either dissolution within PAM or transport within PAM to the mucocilliary escalator. The biological half-time of material in the pulmonary region is very much a function of particulate chemical composition; half-times of hundreds of days have been reported for insoluble particles.

It should be emphasized, however, that dissolution of surface-associated chemical components need not be a requisite for their interaction with the biological system. example, inhaled particles may be phagocytized by macrophages where direct particle ace-cell interaction will take place. A reasonable comparison of "insoluble" cle interaction may be made with asbestos.

In this chapter, the size dependence of physical and chemical properties of coal sh is reviewed. Because the size dependence of many of the chemical properties rom surface-associated chemical phenomena, a detailed description of surface is provided. An understanding of the bioenvironmental significance of ambient requires a detailed understanding of its chemical reactivity and biological tions with fly ash surfaces. This chapter reproduces the material found in a DOE report published through NTIS (Fisher and Natusch, 1979).

II. MORPHOLOGY AND FORMATION OF COAL FLY ASH

A. Morphological Analysis

Morphological studies by light and electron microscopy have described the heterogeneity and structural complexity of coal fly ash. Based on morphological appearance, much can be inferred concerning origin, formation, and chemical composition. McCrone and Delly (1973) indicate that particulate matter derived from combustion products is readily identified under the light microscope. The fused glassy spheres in coal fly ash are the result of exposure to boiler temperatures >1200°C. Aside from the water-white glassy spheres, McCrone and Delly (1973) also describe the presence of opaque "magnetite" spheres and spheres containing trapped gas bubbles.

Light microscopy has been used to define 11 major morphological classes of coal fly ash particles (Fig. 1) in stack-collected, size-fractionated material (Fisher et al., 1978). The characteristics employed in morphological characterization were particle shape and degree of opacity. The 11 classes include (a) amorphous, nonopaque particles, (b) amorphous, opaque particles, (c) amorphous, mixed opaque and nonopaque particles, (d) rounded, vesicular, nonopaque particles, (e) rounded, vesicular, mixed opaque and nonopaque particles, (f) angular, lacy, opaque particles, (g) cenospheres (hollow spheres), (h) plerospheres (sphere filled with other spheres), (i) nonopaque, solid spheres, (j) opaque sheres, and (k) spheres with either surface or internal crystals. A morphogenesis scheme (Fig. 2) has been developed relating the 11 morphological classes to extent and duration of exposure to combustion zone temperatures and probable matrix composition. Opaque amorphous particles and angular, lacy, opaque particles were tentatively classified as unoxidized carbonaceous material or iron oxides (Fisher et al., 1978). Subsequent SEM-x-ray analysis (Fisher et al., 1979a) indicated that these opaque particles were composed of low atomic number matrices. Furthermore, calculation of the effective atomic number of class b particles based upon Bremstrahlung production indicated that this class is predominantly composed of elemental carbon (Fisher et al., 1979b). The opaque spheres (class j) appear to be predominantly magnetite and may be identified by (1) magnetic separation or passing a magnet near a liquid mount of the sample under a microscope and (2) by observation of small clusters of these particles. The amorphous and rounded-vesicular, nonopaque particles (classes a and d) appear to be aluminosilicate particles. Rounding and vesicularity reflect increased exposure to boiler conditions. Further heating of these particles will give rise to nonopaque spheres that are either solid, hollow, or packed with other particles. Similarly, the mixed opaque, nonopaque, amorphous, or rounded classes will give rise to spherical particles upon increased exposure to combustion conditions in the boiler. The nonopaque, solid spheres ranged in color from white to yellow to orange and deep red. Analysis of single particles in this class by SEM-x-ray techniques indicated that the variation in color was associated with iron content (Fisher et al., 1979b). Cenosphere and plerosphere formation will be discussed in detail in the following sections. Crystals within glassy spheres (as determined by light microscopy) are probably formed by heterogeneous nucleation at the surface of the molten silicate droplet (Fisher et al., 1979a). In this regard, Gibbon (1978) has demonstrated the presence of mullite crystals within and on the surface of fly ash particles (Fig. 3). Crystal formation within glassy spheres was demonstrated by transmission electron microscopy (TEM) of hydrofluoric acid-etched replicas. In this process the original glassy material is dissolved, but the insoluble mullite remains. Mullite structure was confirmed by electron-diffraction analysis.

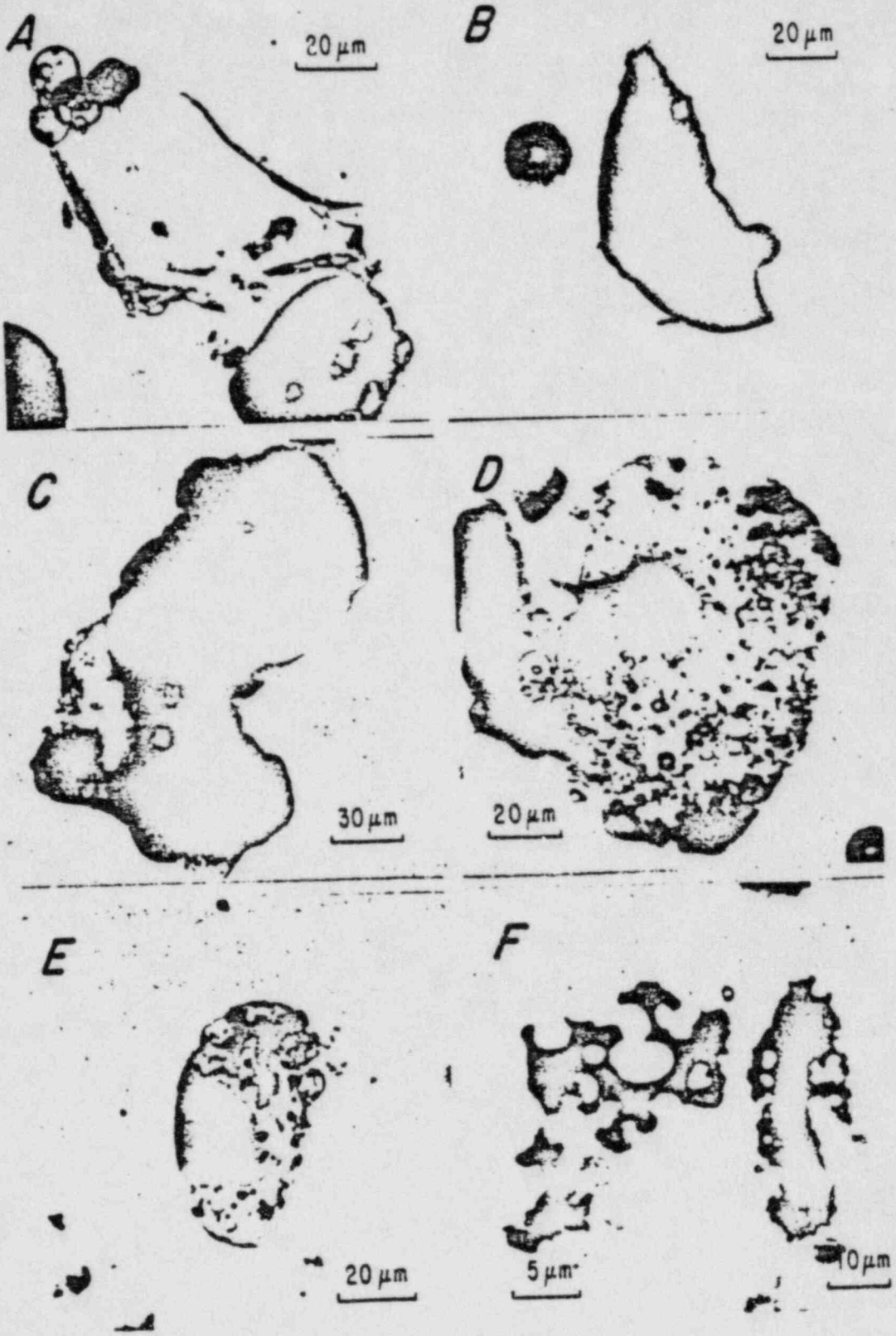
A
20 µm
B
20 µm
C
30 µm
D
20 µm
E
20 µm
F
5 µm
10 µm

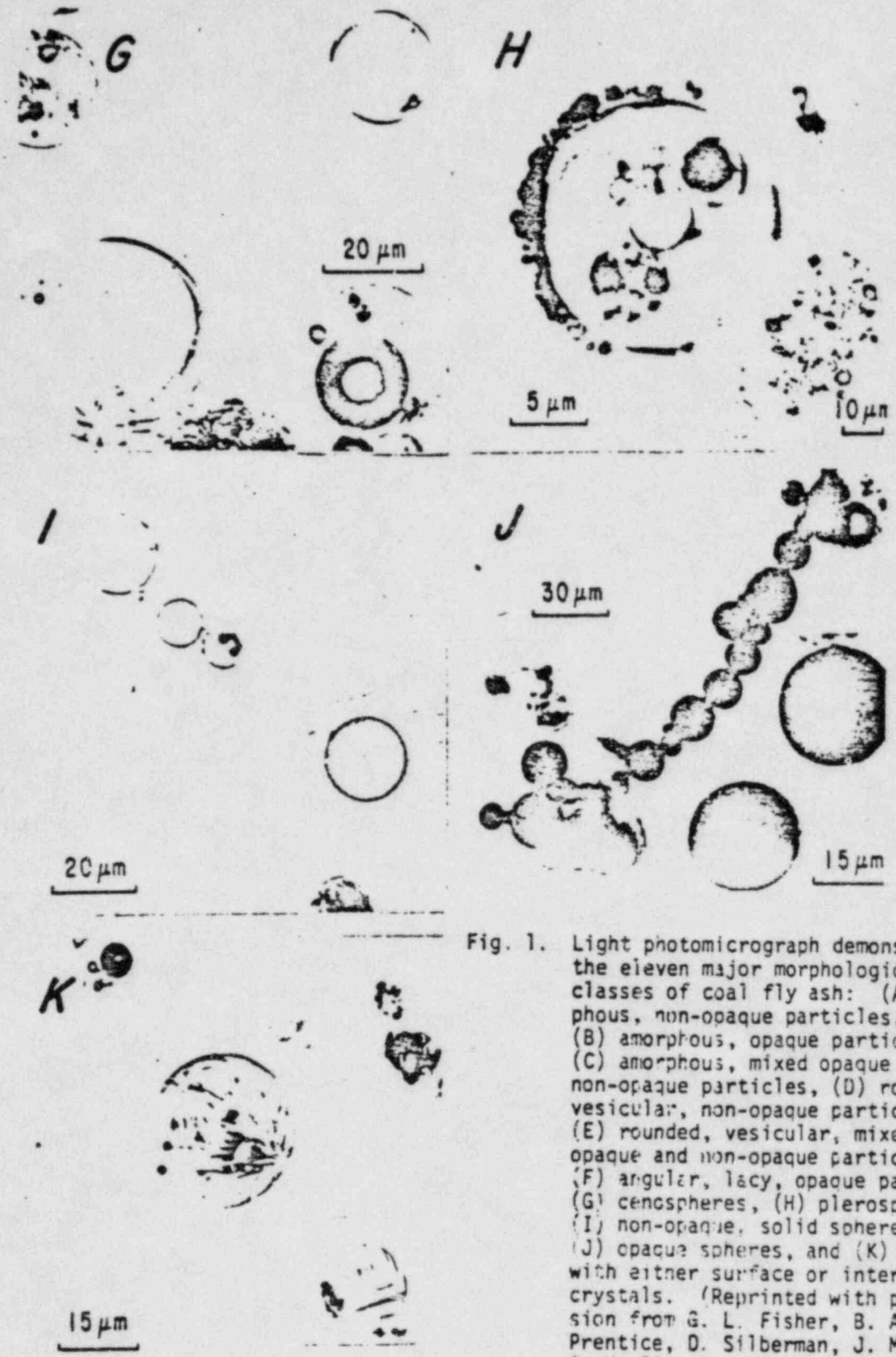

Fig. 1. Light photomicrograph demonstrating the eleven major morphological classes of coal fly ash: (A) amorphous, non-opaque particles, (B) amorphous, opaque particles, (C) amorphous, mixed opaque and non-opaque particles, (D) rounded, vesicular, non-opaque particles, (E) rounded, vesicular, mixed opaque and non-opaque particles, (F) angular, lacy, opaque particles, (G) cenospheres, (H) plerospheres, (I) non-opaque, solid spheres, (J) opaque spheres, and (K) spheres with either surface or internal crystals. (Reprinted with permission from G. L. Fisher, B. A. Prentice, D. Silberman, J. M. Ondov, A. H. Biermann, R. C. Ragaini, and A. R. McFarland, Environmental Science and Technology 12, 449 (1978). Copyright 1978 by the American Chemical Society.)

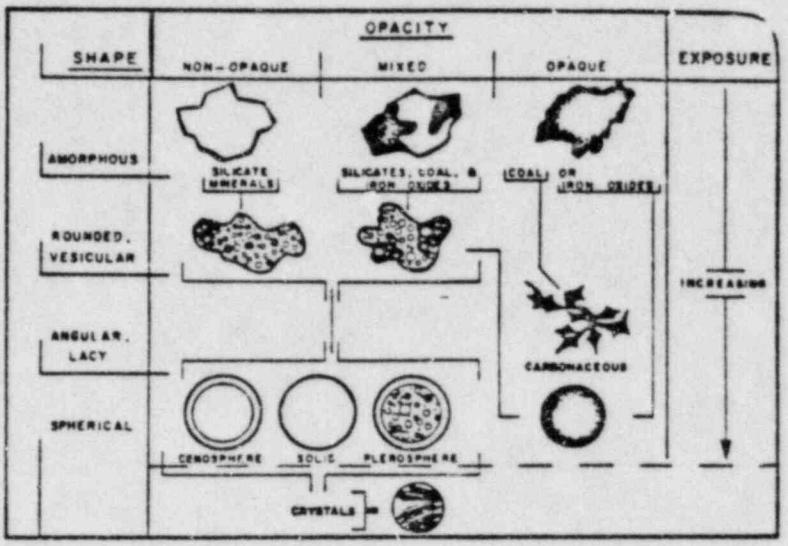

Fig. 2. Fly ash morphogenesis scheme illustrating probable relationship of opacity to particle composition, and relationship of particle shape to exposure in combustion chamber (Reprinted with permission from G. L. Fisher, B. A. Prentice, D. Silberman, J. M. Ondov, A. G. Biermann, R. C. Ragaini, and A. R. McFarland, Environmental Science and Technology 12, 450 (1978). Copyright 1978 by the American Chemical Society.)

Fig. 3. Transmission electron micrograph of a replica of a fly ash sphere showing abundant mullite needles. The association of crystals-within-sphere is retained by the replica; the original glassy material is dissolved during the replication process, but mullite is insoluble in HF. (Photos courtesy of G. A. Waits, D. S. McKay, and D. L. Gibbon, Lyndon B. Johnson Space Center, Houston, Texas.)

Fisher et al. (1978) have quantified the relative abundances of the 11 light-microscopically defined morphological classes in four size-classified, stack-collected fly ash fractions (McFarland et al., 1977). The four fractions had volume median diameters (VMD's) of 2.2, 3.2, 6.3, and 20 μm with associated geometric standard deviations (σ_g) of approximately 1.8 for all fractions. The data in Table I demonstrate that the relative abundances of all particle classes are size dependent. In particular, only the nonopaque solid spheres increased in abundance with decreasing particle size; all other morphological classes appeared to increase in frequency with increasing particle size. Amorphous and vesicular particles (classes a, b, c, d, e, and g) predominated in the coarsest fraction (66% by number), while solid, nonopaque spheres predominated in the finest fraction (87% by number).

Table I. Relative Abundance (%) of Morphologic Particle Classes in Four Fly Ash Fractions[a]

Particle class	Fraction			
	VMD[b] = 20 μm	VMD = 6.3 μm	VMD = 3.2 μm	VMD = 2.2 μm
(A) Amorphous, nonopaque	7.25	2.13	0.79	0.33
(B) Amorphous, opaque	0.42	0.18	--	--
(C) Amorphous, mixed opaque and nonopaque	0.77	0.09	--	--
(D) Rounded, vesicular, nonopaque	12.39	6.67	2.91	2.99
(E) Rounded, vesicular, mixed opaque and nonopaque	2.27	0.24	--	0.03
(F) Angular, lacy, opaque	1.34	0.57	0.27	0.33
(G) Nonopaque, cenosphere	41.11	25.22	13.20	7.91
(H) Nonopaque, plerosphere	0.51	0.21	--	--
(I) Nonopaque, solid sphere	25.58	56.01	79.16	86.99
(J) Opaque sphere	1.56	0.90	0.33	0.24
(K) Nonopaque sphere with crystals	6.80	6.79	3.18	0.95

[a] From Fisher et al. (1978c).

[b] Volume median diameter.

B. Morphogenesis

1. Cenosphere Formation

The mechanism of formation of cenospheres, i.e., hollow spheres, has been the subject of a number of reports. Raask (1966) demonstrated that sphere formation may result from melting of mineral inclusions in coal on a nonwetting surface, namely carbon. He also demonstrated that gas generation inside the molten droplet resulted in cenosphere formation. He reported two stages of gas evolution. In the first stage, directly after melting coal-ash slag, SO_2 and N_2 were released. The SO_2 was thought to result from sulfate decomposition and N_2 from air trapped in the melt. Further heating resulted in CO evolution that was catalyzed by addition of iron or iron oxide to the melt. The author hypothesized that iron carbide was formed at the slag-carbon interface and then reacted with silica resulting in CO evolution:

$$2Fe_3C + SiO_2 \rightarrow Fe_3Si + 3Fe + 2CO \qquad (1)$$

In a subsequent report, Raask (1968) describes the physical and chemical properties of cenospheres in pulverized fuel ash collected by the electrostatic precipitators at 10 power plants. The analysis of major elements indicated that the mass of the cenospheres consisted of 75-90% aluminosilicate, 7-10% iron oxide, and 0.2-0.6% calcium oxide. The mass median diameter of the sieved cenospheres from four power plants ranged from 80 to 110 μm. Raask (1968) analyzed the gas content of the cenospheres after breaking the particles in a hydrogen atmosphere. Approximately 0.2 atm (20°C) of gas composed of CO_2 and N_2 was calculated to be present in each of the four ashes studied. In contrast to his previous work (Raask, 1966), no detectable CO was present. Raask suggested that the source of the CO_2 was the oxidation of carbon by iron oxide:

$$2Fe_2O_3 + C \rightarrow 4FeO + CO_2 \qquad (2)$$

This hypothesis was supported by the observation of a higher $FeO:Fe_2O_3$ ratio in the cenospheres than in the denser ash. He also speculated that cenosphere nitrogen may result from decomposition of silicon nitride:

$$Si_3N_4 + 6Fe_2O_3 \rightarrow 3SiO_2 + 12FeO + 2N_2 \qquad (3)$$

It is also possible that the observed CO_2 evolution was due to carbonate mineral decomposition. Assuming a diameter of average volume of 100 μm, a density of 0.5 g/cm^3 and 0.5% CaO, only 20% of the calcium need be associated with carbonate mineral to provide sufficient CO_2. In this regard, Fisher et al. (1976) have postulated that CO_2 released by crushing fly ash under vacuum (after thorough degassing) was the result of carbonate mineral decomposition, which occurred during coal combustion. In those studies, CO_2 and H_2O were thought to be due to clay mineral decomposition. In particular, based on the stoichiometry of major elements, Fisher et al. (1976) suggested that the major clay mineral in the parent coal (western United States) was kaolinite. In a detailed study of the transformation of mineral matter in pulverized coal, Saroffim et al. (1977) demonstrated that the three major inorganic components in a bituminous coal and lignite were kaolinite, a mixture of calcium carbonate and sulfate, and pyrites. These

authors estimated that the mineral matter in the bituminous coal was 50% kaolinite, 40% pyrite, and 10% calcium sulfate and carbonate, and that in lignite it was 50% kaolinite, 10% pyrite, and 40% calcium sulfate and carbonate. The mass median diameter of the mineral matter was 2 μm for both coals. The optimal temperature for cenosphere formation based on ash density was demonstrated to be 1500°K. This optimum was rationalized by calculating the time for sphere formation. At higher temperatures gas evolution is too rapid and gas will escape from the molten ash; while at lower temperatures sphere formation is too slow relative to the duration of the molten state within the furnaces. Padia et al. (1976) have summarized the principal reactions that take place in mineral matter during coal combustion:

$$Al_2Si_2O_5(OH)_4 \rightarrow Al_2O_3 \cdot 2SiO_2 + 2H_2O, \quad (4)$$

+

$$Al_2O_3 + 2SiO_2, \quad (4a)$$

$$2FeS_2 + 5.5O_2 \rightarrow Fe_2O_3 + 4SO_2, \quad (5)$$

$$CaSO_4 \rightarrow CaO + SO_3, \quad (6a)$$

$$MgSO_4 \rightarrow MgO + SO_3, \quad (6b)$$

$$Fe_2(SO_4)_3 \rightarrow Fe_2O_3 + 3SO_3, \quad (6c)$$

$$CaCO_3 \rightarrow CaO + CO_2, \quad (7a)$$

$$CaMg(CO_3)_2 \rightarrow CaO + MgO + 2CO_2 \quad (7b)$$

These reactions, Eqs. 4-7, all generate gaseous decomposition or oxidation products. Kaolinite decomposition [Eq. (4)], pyrite oxidation [Eq. (5)], calcium and magnesium sulfate decomposition [Eqs. (6a)-(6b)], and calcium carbonate [Eq. (7a)] and dolomite decomposition [Eq. (7b)], may all occur at 1000°C or less, and thus may readily provide gas pressure for cenosphere formation.

2. Plerosphere Formation

Light and electron microscopic studies have identified a morphological class of spherical particles containing encapsulated smaller spheres (Matthews and Kemp, 1971; Natusch et al., 1975; Fisher et al., 1976) (Fig. 4). These encapsulating spheres or plerospheres (Fisher et al., 1976) are similar to cenospheres in that they are composed of an aluminosilicate shell but are filled with individual particles rather than gas (Fig. 4a-4b). Matthews and Kemp (1971) and Natusch et al. (1975) have established that plerosphere formation is truly the result of encapsulation during particle formation rather than filling of a ruptured cenosphere. For these studies, either the electron beam of a scanning electron microscope (Matthews and Kemp, 1971) or an argon-ion milling apparatus (Natusch et al., 1975) were used to etch through the individual particle surfaces. Subsequent examination of the etched particles indicated the presence of numerous smaller particles within the plerosphere, thus confirming that encapsulation occurred during particle formation.


A


B


C

Plerosphere formation is hypothesized to result from a process similar to cenosphere formation (Fisher et al., 1976). As the aluminosilicate particle is progressively heated, a molten surface layer develops around the solid core (Fig. 4c). Mineral decomposition, with evolution of CO_2 and H_2O, then results in formation of a bubble around the core, which remains attached to the molten shell. Further heating leads to additional gas formation causing the core to boil away from the shell. This process may result in concomitant formation of fine particles. The process can be repeated until the plerosphere is full of other plerospheres or solid particles or until the particle freezes. The characteristic time for formation of a 50-μm-diam plerosphere was calculated to be about 1 msec. Similarly, Raask (1968) calculated the formation time of a 50-μm cenosphere to be about 0.3 msec.

3. Surface Crystal Formation

Surface crystals (Fig. 5) identified by SEM have been explained by reaction of sulfuric acid with metal oxides (Fisher et al., 1976). This crystal formation process is relatively slow compared to the time required for particle formation. Fisher et al. (1976) have hypothesized that surface crystal formation results from SO_2 hydration and subsequent oxidation on fly ash surfaces to form H_2SO_4, which then reacts with metal oxides, predominantly CaO, or with ambient NH_3 to form either $CaSO_4$ or $(NH_4)_2SO_4$. Such a mechanism could also result in formation of soluble compounds from relatively insoluble oxides, e.g., conversion of PbO to $PbSO_4$. Fine particulate matter has also been observed by SEM on fly ash surfaces by a number of investigators (Cheng et al., 1976; Fisher et al., 1976, 1978; Matthews and Kemp, 1971; Natusch et al., 1975; Sarofim et al., 1977; Small, 1976). Small (1976) has identified four surface morphologies based on SEM analysis (Fig. 6). Spheres with smooth surfaces comprised the most commonly encountered particle morphology (Fig. 6a). Spheres with small surface particles (Fig. 6c) or relatively large surface-associated droplets, resulting from condensation and solidification (Fig. 6b), were also observed. Elemental analysis of these two particle classes indicated the surface was predominantly Si and Al and the underlying particle was mainly Fe. A fourth class of spherical particles with high Fe concentrations was found to display an unusual pattern of coarse surfaces (Fig. 6e). Sarofim et al. (1977) reported the presence of submicron silica particles on laboratory-generated fly ash. As an extension of the vaporization-condensation mechanism of Davison et al. (1974) for trace elements, Sarofim et al. (1977) suggest that silica deposition resulted from formation of fine silica particles that agglomerate on fly ash surfaces. The formation of submicron silica particles was thought to be because of nucleation of SiO resulting from reaction of SiO_2 with carbon.

4. Spherule Formation from Natural Processes

It is interesting to note the natural (nonanthropogenic) occurrence of glassy spheres with morphological appearance similar to fly ash. Glassy spherules have been reported to be present on shatter cone surfaces (Gay, 1976). These spherules were presumed to be the result of meteorite impact. Similarly, glassy spheres have been

10 µm
A
2 µm
B
25 µm
C
3 µm
D
12 µm
E
F
1 µm

identified in lunar dust samples. Nagy et al. (1970) reported the presence of fine glass beads that were either spherical, nearly spherical, or dumbbell shaped in Apollo II lunar samples. Some broken glass beads were hollow and vesicular, similar to cenospheres; particle surfaces generally were coated with fine particulate matter. CH_4, CO, and CO_2 were found to be entrapped in the glass beads. Carter and MacGregor (1970) reported that glass spheres ranged in color from colorless through green, brown, wine-red, to opaque. In discussing the formation of the lunar spherules, Gibbon (1976) pointed out that the morphology is related to either impaction or volcanism. The loose lunar soil is primarily composed of spherical particles, indicating a high-temperature origin. Waits et al. (1978) have performed detailed morphological studies of lunar samples from the Apollo 17 and the Russian Luna missions (Fig. 7). Smooth vesicular spheres (Fig. 7a) and spheres with internal vesicles have been identified. Fine particulate matter on sphere surfaces (Fig. 7b) is thought to reflect the in-flight aggregation of fine particles on molten sphere surfaces. Knobby spheres (Fig. 7c) that are predominantly crystalline are thought to be feldspar. Detailed surface analysis of some lunar spherules indicate submicron crystals with lath-shaped habit (Fig. 7d). Plerospheres have also been observed (Figs. 7e and 7f), although it is not known whether particles in the plerospheres of Figs. 7e and f filled a fracture after vesicle formation or were formed inside the sphere. Thus it appears that studies of coal fly ash formation and lunar spherule formation are complementary and should provide mutual support in understanding the physical and chemical processes involved in the high-temperature morphogenesis of particulate matter.

III. PHYSICAL PROPERTIES OF COAL FLY ASH: PARTICLE SIZE DEPENDENCE

In addition to particle morphology, a number of other physical properties have been investigated in attempts to elucidate the formation and behavioral characteristics of fly ash. Such properties include the mass distributions of particle size and the particle density, specific surface area, electrical resistivity, and ferromagnetic susceptibility. Unfortunately the available data are sparse and apply to fly ash collected after a control device or from the device itself. Consequently, it is not presently possible to relate physical properties to parameters such as plant operating conditions or the type of coal from which the fly ash was derived. Nevertheless, it is qualitatively apparent that the physical properties of fly ask depend upon both of these parameters.

A. Mass Distribution

Measurements of the distribution of fly ash particle mass with size are of two distinct types. The first involves determination of the aerodynamic particle size distribution, which normally involves isokinetic collection of fly ash directly from a stack gas stream. Several sampling devices are available, but the most common involve the principle of inertial impaction and enable collection and size classification of fly ash in situ. The principles and methodology of inertial sampling have recently been reviewed by Raabe (1976), Newton et al., (1977) and Natusch et al. (1978). Alternatively,

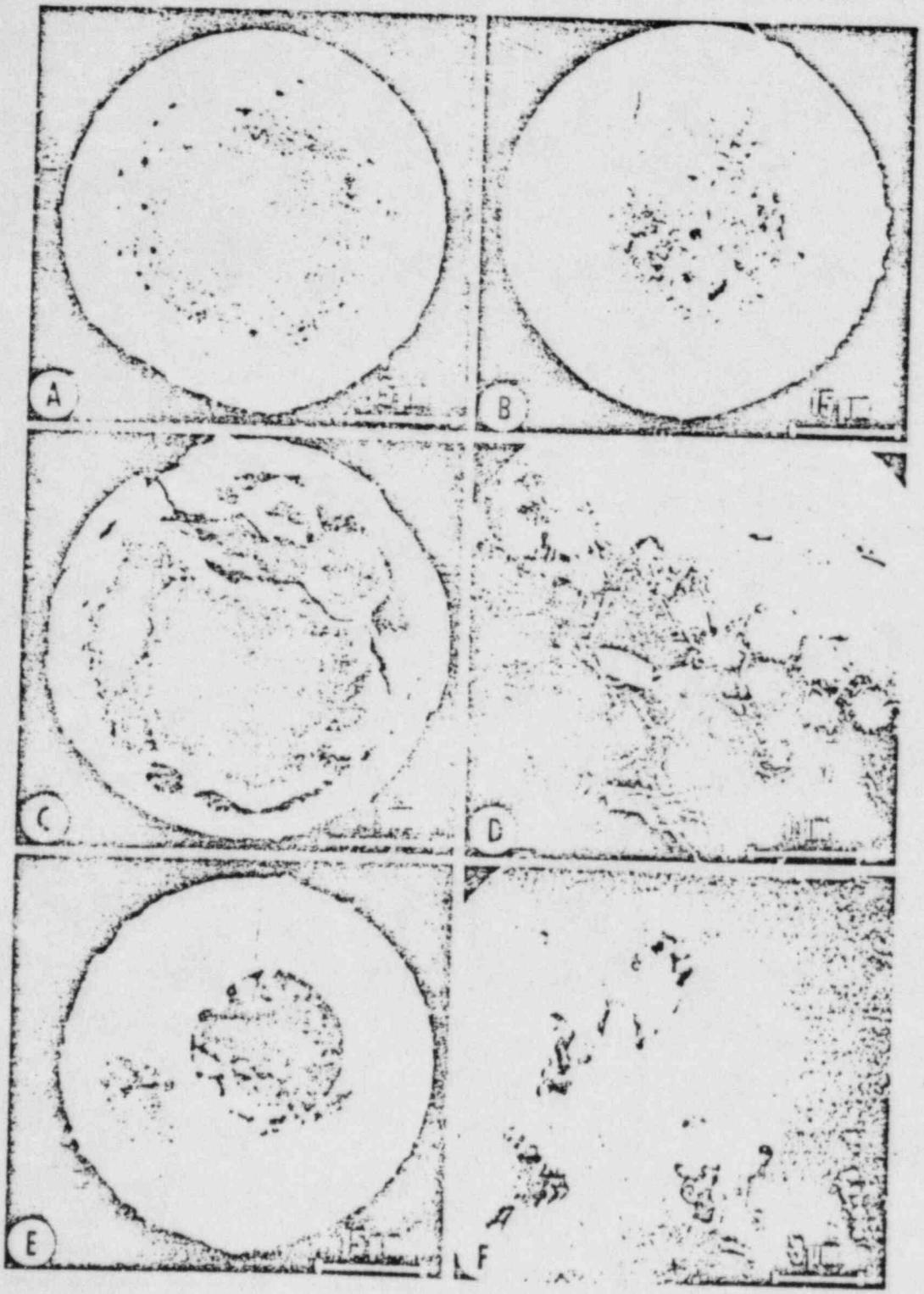

Fig. [illegible] ...les from the U. S. Apollo 17 and the ...ular sphere, and Sphere with aggregate ...ence detail indicating sub-micron, ...with-rock mare (intersphere) structure. ...ay and D. L. Gibson, Lyndon B. Johnson

bulk fly ash, such as might be collected from an electrostatic precipitator or bag house, can be differentiated into physical size fractions by mechanical sieving. In either case, it is necessary to separate the various size fractions prior to weighing or microscopic counting for size estimation.

These two types of measurement are quite distinct. Aerodynamic size determination enables prediction of the atmospheric and airstream behavior of each size fraction, such as is important for establishing particulate collection efficiency, atmospheric residence, and inhalation characteristics (White, 1963; Butcher and Charlson, 1972; Natusch and Wallace, 1974; Yeh et al., 1976). On the other hand, physical size determination provides a straightforward measurement of the physical dimensions of the particles and can be directly related to particle number. Interconversion between aerodynamic and physical sizes can be accomplished using the relationship (Koltrappa and Light, 1972):

$$D_{ae}^2 = D_r^2 C(D_r)\rho_r / C(D_{ae})\rho_{ae} \qquad (8)$$

D_{ae} is the aerodynamic particle diameter, D_r is the physical particle diameter, ρ_r is the particle density, ρ_{ae} is 1 g/cm^3 by definition, and $C(D_{ae})$ and $C(D_r)$ are the Cunningham slip correction factors for the diameters D_{ae} and D_r. Raabe (1976) has compared the commonly used conventions for description of the aerodynamic size of respirable aerosols, including a detailed description of the slip correction and dynamic shape factors. Aerodynamic size distributions are often presented as log-normal probability functions of the grouped mass or number data derived from inertial impaction instrumentation. The general mathematical approach to fitting size distributions to aerosol data has recently been described by Raabe (1978).

Despite the comparative simplicity of determining both the aerodynamic and physical size distributions of fly ash mass, the number of available measurements of fly ash prior to collection by control equipment is relatively sparse. It has been established, however (Southern Research Institute, 1975), that the size and morphology of fly ash depend not only on the nature of the mineral inclusions in coal, as discussed in the previous section, but also on the manner in which the coal is burned. This latter dependence is illustrated in Fig. 8 for fly ash derived from coal burned in a chain grate stoking unit, a pulverized coal fed unit, and a cyclone fired unit (Southern Research Institute, 1975). In each case the fly ash was sampled upstream from control equipment so it is representative of that generated by combustion.

It is apparent from Fig. 8 that the fly ash mass approximates a log-normal distribution over the aerodynamic size range considered. Furthermore, although the geometric standard deviations of the three distributions are similar, their mass median diameters differ considerably (i.e., Cyclone ≈ 6 μm; Pulverized ≈18 μm; Stoker ≈42 μm). These observations are in accord with the general principles of particle formation outlined in the previous section.

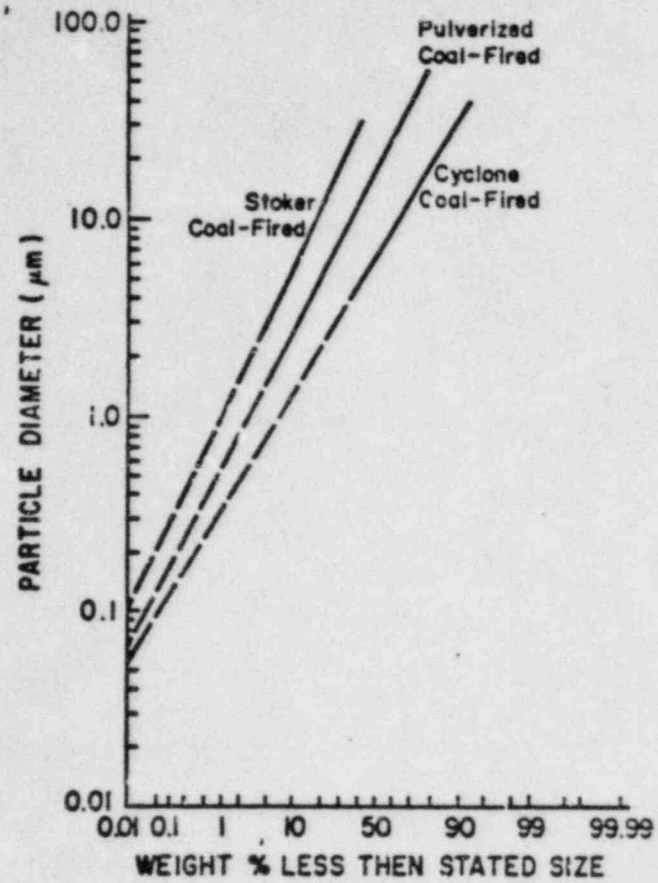

Fig. 8. Size distributions for boiler particulate emissions from coal combustion in a chain grate stoker, a pulverized coal fed unit and a cyclone fired unit. (Reproduced by permission of Southern Research Institute, 1975, and Electric Power Research Institute.)

From a practical standpoint, one is primarily interested in the aerodynamic size distribution of the fly ash that is actually emitted from a coal-fired power plant. This is, of course, largely determined by the collection efficiency of the particle control equipment. Specifically, the size distribution of the emitted fly ash is determined by the product of the functions describing the size dependence of fly ash mass entering a control device and describing the dependence of collection efficiency of this device on particle size. Examples of the aerodynamic size distribution of fly ash mass emitted from a coal-fired power plant equipped with different control devices are presented in Fig. 9.

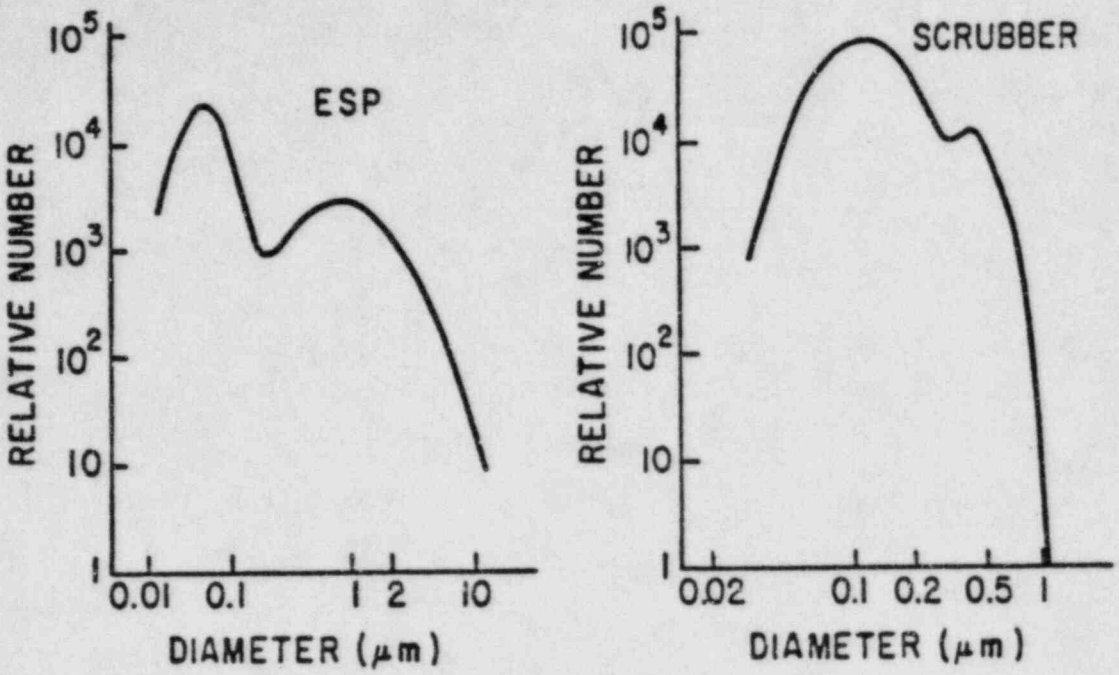

Fig. 9. Size distributions for particulate emissions from similar production units with either electrostatic precipitator (ESP) or a Venturi wet scrubber at the same power plant (Modified with permission from Ondov, et al. 1976).

B. Density and Magnetic Distributions

Determination of the density of coal fly ash as a function of particle size is largely of interest in obtaining an understanding of aerodynamic behavior and of the factors responsible for the intrinsic heterogeneity of coal fly ash. Thus, determination of the densities of different fly ashes, and subfractions thereof, provides a means of interconverting aerodynamic and physical sizes according to Eq. (8). In addition, some differentiation between distinct morphological and compositional characteristics can be achieved. For example, cenospheres can readily be distinguished from solid particles on the basis of density as can predominantly carbonaceous particles from aluminosilicates.

Determination of fly ash particle density is most simply achieved by means of the traditional "float-sink" method that employs a series of liquids of different densities to separate particles of greater and lesser density than the liquid (Ruch et al., 1974; Olsen and Skogerboe, 1975). Alternatively, separation can be achieved by placing the particles in a liquid in which a density gradient has been established.

While determination of particle density is of considerable interest in its own right, more definitive insights are obtained if density separations are carried out in conjunction with sequential size separations and with differentiation between ferromagnetic and nonferromagnetic particles. Such a three-dimensional fractionation scheme has been presented by Natusch et al. (1975), and resulting mass distributions are presented in Tables II and III for fly ashes derived from typical midwestern United States

Table II. Mass distribution of size-classified, magnetic and nonmagnetic fractions of a midwestern bituminous coal fly ash (%) [a]

Size	Density (g/cm^3)											
	Nonmagnetic						Magnetic					
(μm)	<1.6	1.6-2.0	2.0-2.3	2.3-2.7	2.7-3.0	>3.0	<2.1	2.1-2.5	2.5-2.9	2.9-3.4	3.4-3.6	>3.6
<20	b	b	0.2	28.0	b	b	b	0.6	0.4	1.3	14.9	0.5
20-60	1.4	1.3	12.1	12.9	0.1	b	0.2	0.6	1.8	11.5	3.1	0.1
60-90	0.7	1.0	0.6	1.1	0.6	0.1	0.5	0.8	1.0	0.2	b	b
>90	0.1	0.1	0.1	0.6	0.5	0.2	0.1	0.2	0.3	0.2	0.1	b

[a] From Natusch (1978c), unpublished results.

[b] Less than 0.05%.

Table III. Mass distribution of size-classified, magnetic and nonmagnetic fractions of a western sub-bituminous coal fly ash (%)[a]

Size	Density (g/cm^3)											
	Nonmagnetic						Magnetic					
(μm)	<1.6	1.6-2.0	2.0-2.3	2.3-2.7	2.7-3.0	>3.0	<1.6	1.6-2.0	2.0-2.3	2.3-2.7	2.7-3.0	>3.0
<20	b	b	b	0.7	b	b	b	b	b	b	b	b
20-44	0.2	0.4	0.5	21.3	0.3	0.2	b	b	b	1.0	b	b
44-74	0.5	0.8	1.0	45.6	0.6	0.5	0.1	0.1	0.2	6.8	0.1	0.1
>74	0.2	0.3	0.4	16.1	0.2	0.2	b	b	b	1.5	b	b

[a] From Natusch (1978c), unpublished results.

[b] Less than 0.05%.

bituminous and western sub-bituminous coals. These data were obtained by separatio bulk fly ash into several physical size fractions by sieving. Each size fraction wa then subdivided into a number of density fractions that were, in turn, separated into magnetic and nonmagnetic fractions according to whether the particles adhered to a magnet or not. The designation of magnetic and nonmagnetic is entirely operational in nature.

A number of characteristics of coal fly ash can be distinguished from the data presented in Tables II and III. It is apparent that both fly ashes are compositionally extremely heterogeneous, although there are very considerable differences between the mass distributions for these two fly ashes. As discussed in the previous section, much of the variation in densities observed is attributable to morphological rather than compositional characteristics. This is rather well illustrated by the data in Fig. 10, where density distributions have been determined as a function of particle size both before and after crushing the fly ash. The observed shift to higher density on crushing indicates the presence of vesicular particles and cenospheres in the larger size fractions, as discussed previously.

Interestingly, determination of the x-ray powder diffraction patterns of each of the subfractions presented in Tables II and III reveals no convincing differences in matrix composition that depend upon either size or density (Natusch et al., 1975). This finding further supports the contention that the density distributions in fly ash are largely determined by morphology rather than by composition. There are, however, very distinct differences between the amount of magnetite (Fe_3O_4) present in the magnetic and nonmagnetic fractions (Fig. 11). This suggests that magnetite is primarily responsible for the ferromagnetic susceptibility of coal fly ash.

C. Electrical Resistivity Distribution

The electrical resistivity of coal fly ash is an important physical property from the standpoint of control. Thus, it has been established (Bickelhaupt, 1974, 1975) that the collection efficiency of electrostatic precipitators increases with decreasing fly ash resistivity. Bickelhaupt (1974, 1975) has further shown that both the surface and volume resistivities of fly ash, at precipitator operating temperatures, are inversely proportional to the specific concentrations of alkali metals, which are thought to act as charge carriers. These studies have shown that considerable differences in electrical resistivity occur between different fly ashes, and correlations are observed between fly ash resistivity and alkali metal content, but no measurements have been made relating resistivity directly to particle size.

Some insight into the dependence of resistivity on particle size can be obtained by considering the data presented in Table IV. This table lists concentrations of potassium measured in fly ash that has been fractionated sequentially according to size, density, and ferromagnetism as described previously. It can be seen that in the nonmagnetic fractions (that account for 64% of this fly ash) there is a pronounced increase in the concentration of potassium (and also of sodium), both with decreasing particle size and with decreasing density. This suggests that, for this fly ash sample,

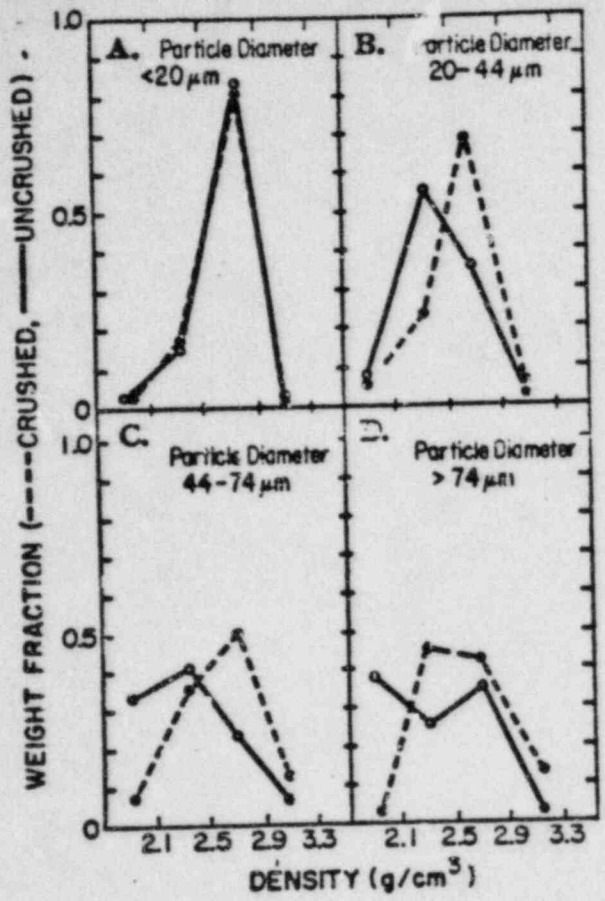

Fig. 10. The effect of crushing on the mass distribution of size-classified fly ash fractions. The shift to higher densities indicates the presence of hollow or vesicular particles (figure by courtesy of D. F. S. Natusch).

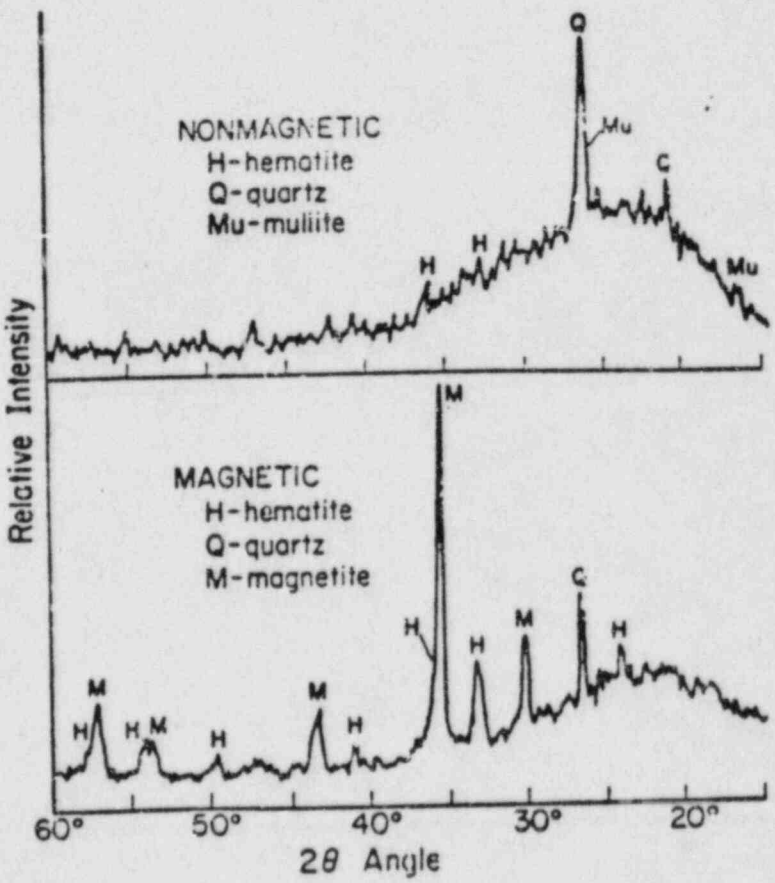

Fig. 11. X-ray powder diffraction patterns demonstrating the compositional differences between magnetic and nonmagnetic fly ash fractions (figure by courtesy of D. F. S. Natusch).

Table IV. Concentration (%) of Potassium in Fly Ash Separated Sequentially by Size, Density, and Ferromagnetism[a]

Particle type	Particle size (μm)	Density (g/cm^3) <2.1	2.1-2.5	2.5-2.9	>2.9
Nonmagnetic	<20	2.69	2.34	2.22	1.73
	20-44	2.63	2.28	1.33	1.09
	44-74	1.39	1.63	1.05	0.45
	>74	1.79	1.48	1.06	0.13
Magnetic	<20	--[b]	--	0.76	0.70
	20-44	--	1.92	1.48	0.73
	44-74	1.78	1.60	1.27	0.85
	>74	1.37	1.62	1.49	0.83

[a] From Natusch et al. (1975).

[b] No meaningful data.

resistivity decreases with particle size and with density. Similar, though less pronounced, density dependencies are observed in the magnetic fractions, but size dependencies, if any, are obscure. Since both decreasing density and decreasing physical size contribute to decreasing aerodynamic size, it is apparent that the efficiency of electrostatic precipitation per unit mass of these size-classified fly ashes increases with decreasing aerodynamic particle size. This is an extremely desirable characteristic. It should be pointed out, however, that these studies require extension to respirable particle sizes.

D. Surface Area Distribution

The specific surface area of fly ash particles is an important parameter in determining a number of the behavioral characteristics of coal fly ash. It is the surface area of a particle that determines the number of electrostatic charges that can be placed on that particle in an electrostatic precipitator (White, 1963; Bickelhaupt, 1974, 1975); it is the surface area of a particle that determines the extent of condensation or adsorption of species from the gas phase (Davison et al., 1974, Natusch and Tomkins, 1977); and it is the surface area of fly ash that determines the rate and extent of its aqueous leaching (Natusch et al., 1975; Matusiewicz and Natusch, 1979).

To a reasonable approximation, one would expect the specific surface area (square meters per gram) of fly ash to increase linearly with decreasing particle diameter since the particles are predominantly spherical. Similar trends would also be expected for nonspherical particles having similar shape factors (Butcher and Charlson, 1972).

In fact, the expected trend is observed; however, two important points are noted. First, the surface areas that are measured for spherical fly ash particles are considerably greater than those calculated from measured particle diameters. Even taking into account the assumptions inherent in surface area measurements, it appears that coal fly ash has a significant "internal" surface area. This is probably in the form of pores or cracks or a porous surface layer, although, as previously described, surface crystal formation may contribute significantly to the measured surface area. However, several fly ashes show no significant dependence of surface area on particle diameter (Table V), especially for small particles. These data indicate the existence of substantial internal surface area that is effectively proportional to particle volume rather than external surface area. In this regard, it has recently been suggested (Natusch, 1978a) that collisionally efficient condensation processes may result in deposition of material from the gas phase predominantly onto the external particle surface, whereas much less efficient adsorption processes (Natusch and Tomkins, 1977) can deposit gases and vapors on both the internal and external surfaces of a particle.

Table V. Comparison of Measured and Calculated Specific Surface Areas of Size-Classified Fly Ash Fractions[a]

Physical Size (μm)	Measured (m^2/g)	Calculated (cm^2/g)
<45	2.02	>267
45- 63	3.55	191-267
63- 90	2.55	133-191
90-125	2.43	96-133
125-180	1.20	67- 96
>180	3.11	<67

[a] From Kim and Natusch (1978). Unpublished results.

IV. ELEMENTAL COMPOSITION OF COAL FLY ASH: PARTICLE SIZE DEPENDENCE

Studies of the size dependence of the elemental concentration of fly ash can be classified into two categories. The first category consists of those studies that relate the elemental concentration to the particle size of size-classified material. For these studies, sufficient mass of size-classified material is collected to allow gravimetric determination prior to elemental analysis. The second category are the many studies that have employed inertial cascade impactor systems for aerodynamic size classification. Aerosol sampling is performed isokinetically to avoid anomalous alteration of the particle size distribution. Because impactor stages are often coated with sticky adhesive to prevent particle bounce off and reentrainment effects and because only small masses of material may be collected on the stages, accurate gravimetric determination of sample mass is difficult. To obviate this complication, specific elemental masses of deposited particles on each stage are often ratioed to the mass of an element that does not demonstrate a marked concentration dependence with particle size. In this regard, Ondov et al. (1977a) have analyzed four size-classified, stack-collected fly ash samples ranging in particle size (VMD) from 2.2 to 20 μm (McFarland et al., 1977). The elements Al, Si, Ca, K, Ce, La, Rb, Nd, Hf, Sm, and Cs varied in concentration by less than 20% among all fractions and should therefore be suitable for mass estimation. A second approach that has been used in the analysis of impactor data, reports the size distribution for the mass of each element analyzed, thus avoiding the compounded errors in data derived from elemental ratios. Impactor studies also report elemental concentrations in terms of mass per unit volume of aerosol sampled. Thus, because of the limitation of gravimetric determination, results from impactor studies are often reported as ratios of elemental masses or mass-to-volume ratios rather than specific concentrations.

Many studies employ the enrichment factor (EF) of Gordon and Zoller (1973). The EF is defined as the ratio of an elemental concentration in the fly ash sample to the elemental concentration in the coal. To provide normalization relative to total mineral content, EF's are often calculated from the ratios of specific elemental contents in the fly ash samples and coal, respectively, to those of mineral matrix elements in the fly ash samples and coal, respectively. Thus, the EF may be calculated from:

$$EF = ([X]_s/[M]_s)/([X]_c/[M]_c), \qquad (9)$$

where $[X]_s$ and $[X]_c$ represent the mass of element X in the sample and coal, respectively, and $[M]_s$ and $[M]_c$ represent the content of the matrix element in the sample and coal, respectively. A number of "matrix" elements have been used in the EF calculation: Al (Gordon et al., 1974), Fe (Ragaini and Ondov, 1977), Sc (Ondov et al., 1977c), Ce (Coles et al., 1979), and ^{40}K (Coles et al., 1978). In the following section, studies of fly ash analyses using gravimetrically determined masses will be discussed separately from studies employing smaller masses.

A number of analytical techniques have been employed in the determination of the elemental composition of coal fly ash. For complete analysis of the major, minor, and trace elements, a combination of analytical techniques is usually employed. The physical and chemical heterogeneity in terms of particle size, chemical distribution within and among individual particles, and the fused aluminosilicate matrix provide a unique combination of difficulties for the analyst. The techniques employed for elemental analysis may be divided into two categories: (1) single element techniques that generally require matrix dissolution and (2) multielement techniques that generally are performed on the undissolved ash. A detailed and extensive review of the elemental analysis of particulate matter has recently been published by Natusch et al. (1978). See also Chapters 11 through 14 in Volume I, and Chapter 46 in this volume.

A. Studies of Specific Concentrations

Davison et al. (1974) published the first detailed elemental analysis of coal fly ash as a function of particle size. The ash was collected from a power plant using southern Indiana coal. Two types of fly ash samples were analyzed: (1) fly ash collected by the plant's cyclonic precipitator and (2) stack-collected material. The precipitator ash was size separated by sieving the larger particles and aerodynamically separating the remaining mass. The stack-collected fly ash was aerodynamically classified using an Anderson impactor. These authors presented the elemental concentrations in three categories based on the degree of concentration dependence on particle size. The elements showing "pronounced" concentration trends of increased concentration with decreasing particle size were Pb, Tl, Sb, Cd, Se, As, Ni, Cr, Zn, and S. Elements classified as showing limited concentration trends were Fe, Mn, V, Si, Mg, C, Be, and Al. Iron concentrations decreased with particle size for the precipitator ash, while no trend was observed in the stack-collected samples. The elements described as showing no concentration trends were Bi, Sn, Cu, Co, Ti, Ca, and K. The mechanism of concentration enhancement has been postulated to be volatilization of the element (or compound) at combustion temperatures (1400°-1600°C) followed by condensation on particle surfaces (Natusch et al., 1974; Davison et al., 1974). Thus, fine particles with their large ratio of surface area to mass will preferentially concentrate volatile inorganic species. In particular, those elements displaying the greatest concentration dependence with particle size generally are associated with elemental forms that boil or sublime at coal combustion temperatures.

Fisher et al. (1977) and Fisher and Chrisp (1978) have described the size dependence of the elemental concentrations in coal fly ash collected from the stack of a power plant burning low-sulfur, high-ash, western United States coal. The fly ash was size classified in situ, downstream from the ESP, using a specially designed instrument employing two cyclone separators in series followed by a 25 jet centripeter (McFarland et. al., 1977). Elements were classified into two categories: elemental concentrations (1) dependent on particle size and (2) independent of particle size. Concentration dependence with particle size was determined qualitatively with the criterion that constant concentration trends beyond experimental uncertainty were observed for each of the four

fractions analyzed. In order of decreasing dependence on particle size, the element Zn, As, Sb, W, Mo, Ga, P, V, U, Cr, Ba, Cu, Be, and Mn displayed increased concentrat with decreasing particle size. Silicon was the only element to decrease in concentratio with decreasing particle size.

The elements not displaying clear-cut concentration dependence on particle size for all fractions analyzed were Al, Fe, Ca, Na, K, Ti, Mg, Sr, Ce, La, Rb, Nd, Th, Ni, Sc, Hf, Co, Sm, Dy, Yb, Cs, Ta, Eu, and Tb. Of these elements, Na, Sr, Ni, and Co displayed marked enhancement in the finest fraction relative to the coarsest fraction. Coles et al. (1979) have described the elemental behavior in the four size-classified fractions in terms of elemental enrichment factors relative to the parent coal.

The elements were grouped into three classes: group I elements displayed little or no enrichment in fine particles and were lithophilic; group II elements displayed marked enrichment and were chalcophilic (sulfur associated); and group III consisted of elements with behaviors intermediate to groups I and II. Group I elements included Al, Ca, Cs, Fe, Hf, K, Mg, Mn, Na, Rb, Sc, Ta, Th, Ti, Ce, Dy, Eu, La, Nd, Sm, Tb, and Yb; group II elements were As, Cd, Ga, Mo, Pb, Sb, Se, W, and Zn; and group III consisted of Ba, Be, Co, Cr, Cu, Ni, Sr, U, and V.

In a separate report, Coles et al. (1978) described enrichment factors for ^{228}Th, ^{228}Ra, ^{210}Pb, ^{226}Ra, ^{238}U, and ^{235}U, relative to ^{40}K in the four size-classified fractions of stack fly ash. Although the EF's for all radionuclides appeared to increase with decreasing particle size, ^{210}Pb, the most volatile radionuclide, showed the greatest size dependence. The authors proposed the U is present as either a carbonate [$Na_2UO_2(CO_3)_2$ or $Na_4UO_2(CC_3)_3$] that upon heating in an oxidative atmosphere may give rise to either volatile UO_3 from oxidation of uranite (UO_2) or the silicate-soluble, nonvolatile mineral, coffinite [$U(SiO_4)_{1-x}(OH)_{4_x}$]. Thus, U behavior would be expected to display an intermediate behavior depending on the relative concentrations of uranite and coffinite. The behavior of Th was rationalized to be due to coexistence in submicron zircon grains in the coal. The authors suggested that ^{226}Ra enrichment may have been due to ^{238}U, while no explanation of ^{228}Ra enrichment was presented.

Campbell et al. (1978) have studied the elemental distribution of size-classified ESP-collected coal fly ash from a western United States power plant. Reaerosolized ESP fly ash was separated into nine size fractions ranging in size (VMD) from 0.5 to 50 μm. The authors describe fine particle enhancement for elements "volatilized during combustion," i.e., As, Co, Cr, Ga, Pb, Se, and Zn. Their data also demonstrate that K, Al, Mn, Mg, Na, Ba, S, Ni, V, Cu, Cs, Rb, Sb, Br, Mo, and Sn display an inverse concentration dependence on particle size. Silicon and possibly Zr were reported to increase in concentration with increasing particle size. The concentrations of Ca and Sr demonstrated a maximum at approximately 5 μm. A similar concentration pattern was reported for Ce, Eu, and Yb.

These studies are in basic agreement with the hypothesis of Natusch et al. (1974) in that the most volatile elements (or their oxides), Cd, Zn, Se, As, Sb, W, Mo, Ga, Pb, and V, displayed the greatest size dependence. Furthermore, the least volatile elements

did not display a strong particle size dependence. With regard to enhancement of Ba and U, Coles et al. (1979) postulated that Ba may form the volatile species $Ba(OH)_2$ and U may be volatilized in part as UO_3. Fisher et al. (1977) have proposed that the presence of Cr in the organic fraction of coal, Mn and Sr as carbonate minerals, and Cu as sulfides, may explain the behavior of these relatively refractory elements. Campbell et al. (1978) speculated that the concentration profiles exhibiting maximum particle sizes of approximately 5 μm for Ca, Sr, and the rare earth elements were because of the presence of these elements in apatite.

B. Studies of Relative Concentrations

Most studies of the chemical properties of size-classified fly ash have employed cascade impactors for stack or plume sampling. Zoller et al. (1974) reported enrichment factors relative to Al for stack-collected fly ash. The ash studied was collected downstream from the ESP at a power plant burning pulverized coal containing 10% ash and 1% S. In agreement with the previously described studies, enhancement of the volatile elements, Sb, Se, As, Pb, Zn, Ni, and I, was observed in the stack fly ash relative to their concentrations in the coal. Bromine was depleted in the stack ash relative to the coal. The authors point out that the EF's for Se, I, and Br are underestimates because portions of these elements were probably in the vapor phase. Elements not displaying enrichments included Ti, Sc, Th, Ta, Na, K, Rb, Mg, Sr, Ca, Ba, V, Cr, Mn, Fe, Co, and six rare earth elements. It should be pointed out that although the stack sample was not size classified, a relatively fine particle distribution (i.e., MMD 5-10 μm) may be presumed for this post-ESP material. In a subsequent report (Gladney et al., 1976), the research team described the size dependency of the EF's in the stack fly ash.

Three patterns of elemental behavior were described. The elements Na, K, Rb, Mg, Ca, Sr, Ba, Sc, Ti, V, Mn, Co, Zr, Th, Hf, Ta, and all rare earths except Ce displayed an EF distribution that was not size dependent. Interestingly, the authors also report that the relatively volatile elements, Cr, Zn, Ni, and Ga, also exhibited little size dependence. A definite increase in EF of fine particles was observed for Pb, As, and Sb. The volatile elements, Se, Br, I, and, to a lesser extent, Hg, displayed bimodal activity. An enrichment minimum was observed from 0.7 to 5.0 μm. Iron and Ce displayed EF's that decreased with decreasing particle size.

Klein et al. (1975) described the pathways of 37 trace elements through a cyclone-fed power plant burning coal of 3% S and 11% ash. Concentration ratios for ESP outlet versus inlet ash indicated enhancement of As, Cd, Cr, Pb, Sb, Se, V, and Zn in the finer fly ash fraction. The authors point out that the ESP efficiency was 96.5% during their first sampling trip, as compared to 99.5% during their second sampling trip. Interestingly, the removal of the major elements was more complete during the second trip, although no change in capture efficiency was observed for Cd, Pd, and Zn because of association with fine particles. The authors estimate that 60-90% of the Hg was released from the stack as a vapor. In a subsequent study, Andren and Klein (1975) presented extensive data on the mass balance and chemical form of selenium emissions from the same power plant. The authors concluded that 68% of the Se was incorporated into fly ash. Based on an ESP efficiency of 99.6%, the authors also concluded that 93% of the

Se released to the environment is in the vapor phase. The oxidation state of Se was determined to be Se^0 based upon inefficient extraction in HCl and complete elemental extraction in Br/Br^--redox buffer, 16M HNO_3, 18M H_2SO_4, or 1:1 HNO_3:$HClO_4$.

Mercury emissions from coal-fired power plants have been described in detail. Billings and Matson (1972) and Billings et al. (1973) studied mercury emission from a power plant burning low sulfur (<1%), high ash (21%) pulverized coal. The authors concluded that 90% of the Hg was released from the stack as a vapor and that fly ash particles represented less than 1% of the Hg emissions. The annual release of Hg from all coal-fired United States power plants was estimated to be 10^3 metric tons in 1971. Similarly, Diehl et al. (1972) studied Hg emissions from a 100-g/hr pulverized coal combustor and a 500-lb/hr pulverized coal combustor. Although these authors experienced difficulties in their collection of Hg from the flue gas, 35 and 60% of the total Hg was found in the fly ashes generated from combustion of coals having ash contents of 21.6 and 6.9%, respectively, and sulfur contents of 5.2 and 1.2%, respectively. Subsequent studies in the larger combustor using coal with 10.1% ash and 2.1% S, resulted in fly ash containing 12% of the total Hg. The authors present calculations for two Illinois power plants, indicating that the Hg content of ash contained within the plants accounted for 7 and 19% of the total Hg in the coal. Thus, in agreement with Billings' work, most of the Hg in coal is volatilized and released as a vapor to the atmosphere. Similarly, Kalb (1975) has reported that the major portion of Hg in coal is volatilized during combustion and released to the atmosphere. Approximately 10% of the volatilized Hg was found to be adsorbed onto fly ash; organomercury compounds were not observed. The author points out that Hg emissions could be reduced by coal cleaning, which results in removal of higher density minerals, including pyrite that is relatively high in Hg contents.

In a review of trace element studies related to low sulfur, high ash coal combustion in Four Corners, New Mexico, Wangen and Wienki (1976) described enrichment factors for electrostatic precipitator ash relative to bottom ash. Enhancement in the precipitator ash was observed for the following elements in order of decreasing magnitude: Se, As, F, Sb, Zn, Tl, Hg, Mo, Ga, B, Pb, V, and Cr. Enrichment factors near unity were observed for the other 22 elements studied.

Kaakinen et al. (1975) studied the behavior of 17 elements in the inlets and outlets of a power plant burning pulverized coal containing 0.6% S and 6% ash. Although particle size was not reported, the author described the specific surface area of his samples. The surface areas measured by nitrogen adsorption for the bottom ash, mechanical collector hopper ash, electrostatic-precipitator hopper ash, and electrostatic-precipitator-outlet fly ash were 0.38, 1.27, 3.06, and 4.76 m^2/g, respectively. Enhancement in trace element concentration relative to Al was observed for Pb, Mo, As, Zn, Sb, and Cu.

The magnitude of the EF's correlated with relative distance of each outlet downstream from the boiler and the specific surface area of the ashes. The authors point out that As enrichment depends on the Ca content of the coal; As_2O_3 is associated with low Ca coals while As_2O_5 is associated with high Ca. Zirconium was the only element displaying a decrease was thought to be because of the occurrence of Zr as zircon, a relatively high densith mineral that may be more efficiently captured by the mechanical collector. Contrary to this observation, little or no enrichment was reported for Nb, Sr, Fe, Rb, and Y.

Ondov et al. (1977b,c) have performed extensive analyses of element enrichments in fly ash as a function of particle size. In the study of two large western power plants burning high ash, low sulfur, pulverized coal, Ondov et al. (1977c) reported considerable enrichment of W, U, Ba, Zn, V, In, Ga, Br, As, Se, Sb, and Mo in fine particles for the plant with an ESP rated at 99.5% efficiency. In the second plant, with a 97% efficient ESP, EF distribution tended to be bimodal for these elements, with a broad maximum of 2-10 μm. The authors also point out that Br, Se, Cr, Mn, Ta, Co, and Zn displayed enrichment in both the fine and the large particles, i.e., an EF minimum was observed from approximately 1 to 8 μm. The authors indicate that the biphasic distributions may be the result of artifacts in collection because the larger particles will be collected on the first impactor stages, through which vapor containing volatile elements is initially drawn.

Fisher et al. (1979d) also reported data supporting bimodal elemental distributions. Filtration studies with neutron-activated, stack-collected fly ash (VMD = 2.2 μm; σ_g = 1.8) were performed by dispersing ash samples in buffer at pH 7.4 and filtering through a membrane with pore size of 5, 2, 0.8, 0.4, 0.2, 0.1, 0.05, or 0.03 μm. The elements were classified into four groups based on their behavior: (1) Na, Ca, Co, Se, Mo, and Ba were partially soluble and did not display filtrate concentrations that were pore-size dependent; (2) Sb, As, Zn, W, Cr, and U displayed a pattern of filtrate concentrations that appeared to be bimodal; (3) K, Si, Fe, Ce, Sm, Eu, and Th were only detected in filtrates from membranes >2 μm in pore size; and (4) Zr, Cs, Nd, Rb, Tb, Yb, Hf, and Ta were not detected in the filtrates. For those elements displaying bimodal behavior, a relatively large increase in concentration was observed in filtrates derived from the 0.4 μm membrane. The concentration profile remained constant thereafter. These data suggest a concentration maximum for Sb, As, Zn, W, Cr, and U in fine particles less than 0.4 μm in diameter.

Ondov et al. (1977c) have compared enrichment factors for the two power plants to those published by Klein et al. (1975), Kaakinen et al. (1975), and Gladney et al. (1976). The comparison (Table VI) for EF's for elements in stack-collected fly ash indicates relatively good agreement between studies of different power plants with ESP control systems employing a wide variety of coals. In light of the uncertainties, only Mo, Se, and Mn showed significant differences between plants. The volatile elements Sb, As, and Pb were clearly enhanced in samples from all power plants; Zn, Se, Cr, and V were enhanced in stack ash from those plants with the most efficient ESP's, i.e., those plants presumably releasing the finest ash. Bromine was the only element displaying a significant fractional EF. Ondov et al. (1977c) point out that the EF's for stack ash collected from a unit with a venturi wet scrubber (VWS) are generally much higher than those for plants with ESP's. The authors attribute these findings, in part, to the high efficiency (>99%) of removal of particles >2 μm and the low efficiency (40%) of removal of particles <2 μm by the VWS. In another study, Ondov et al. (1979b) indicated that the ratio of VWS-to-ESP fractional emissions of submicron, supermicron, and total suspended particles were 1:6, 11:1, and 10:1, respectively. They also proposed that

Table VI. Enrichment Factors for Elements in Stack Fly Ash from Coal-Fired Power Plant

	Western U.S. plant A[b]	Western U.S. plant B (ESP)[c]	Allen Steam plant[d]	Chalk point[e]	Valmont[f]	Western U.S. plant C (VWS)[g]
Sb	7.0	5.3	6.7	4.0	--	120
Cd	--	6.0	--	--	--	--
W	--	4.9	--	--	--	70
As	6.6	7.9	6	6.3	--	100
In	5.5	3.7	--	--	--	20
Zn	4.3	4.3	7.8	1.5	2.5	19
Pb	--	3.8	8.1	3.7	3.1	--
Ga	4.3	3.0	--	1.2	--	--
U	3.3	2.5	--	--	--	13.5
Se	3.0	5.3	5.5	5.7	1.7	400
Ba	2.5	2.7	0.7	0.92	--	13
Cr	2.3	2.6	3.0	1.1	--	100
Co	2.3	1.7	1.4	1.0	--	4.3
V	2.0	2.5	2.5	0.75	--	21
Mo	1.8	3.5	--	--	3.0	43
Mg	1.1	0.8	0.54	--	--	2.7
Fe	1.1	0.90	0.84	0.83	1.0	2.0
Na	1.0	1.1	0.99	--	--	3.2
Sc	1.0	1.0	1.0	1.0	--	1.0
K	1.0	0.7	0.95	0.83	--	0.86
Th	0.95	0.90	0.76	--	--	0.89
Al	0.86	0.75	0.44	0.83	0.94	1.3
Ca	0.76	0.89	--	0.92	--	7.6
Mn	0.68	1.1	0.78	--	--	21
Be	--	0.6	--	0.64	--	--
Br	0.2	0.1	--	0.17	--	57

[a] Modified from Ondov et al. (1977c).

[b] Plant A employed an ESP with removal efficiency of 99.6% (Ondov et al., 1977c).

[c] Plant B employed an ESP with efficiency of 97% on one unit and a venturi wet scrubber (VWS) on a second unit (Ondov et al., 1979).

[d] Employed an ESP with 99.5% efficiency (Klein et al., 1975).

[e] Employed an ESP with 75% efficiency (Gladney et al., 1976).

[f] Employed a mechanical collector and an ESP with 91% efficiency (Kaakinen et al., 1975).

corrosion may enhance VWS emissions of Cr, Co, Cu, and Zn. Thus, although the VWS may have a higher removal efficiency of total suspended particulate matter, the ESP may more efficiently remove respirable particles.

Ondov et al. (1977b) have reported enrichment factors for plume samples collected from a power plant with five generating units, of which two units were equipped with ESP's and the other three with VWS's. Elemental enrichment factors were relatively constant as a function of distance from the stack for Sc, Na, K, Cu, and the lanthanides. Enrichments for Mo, V, Ba, U, Ga, In, As, W, and Se increased from the stack to the plume. Subsequent plume samples indicated decreased EF's with distance from the point of release. The only elements displaying increased enrichments with increased distance from the stack were Br, Sb, Zn, and Co. The increased EF for Br was postulated to be because of mixing of plume aerosols with high background concentrations of Br, possibly because of automotive sources (Ondov et al., 1977b).

In a further comparison of the stack fly ash from an ESP unit with that from a VWS unit, Ondov et al. (1979b) reported that the mass median aerodynamic diameters (MMAD's) for the elements As, Ba, Sb, Se, U, V, and W in the ESP ash were approximately tenfold higher than in the VWS ash, which ranged from 0.47 to 0.59 μm. The authors concluded that despite an eleven-fold higher total particulate emission, the ESP unit is far more efficient at removing submicron particles than is the VWS unit. Thus, the scrubber unit tested appeared to be less effective at reducing potential inhalation hazards than the precipitator unit.

C. Surface Deposition Models

A number of investigators have presented mathematical models relating the concentrations of relatively volatile elements to geometric parameters associated with fly ash particles. Assuming a volatilization-condensation mechanism, Davison et al. (1974) proposed a simple mathematical model for elemental concentration as a function of particle size. Their model predicts that the elemental concentration of a volatile species will be inversely dependent on particle size. Kaakinen et al. (1975) presented a similar mathematical dependence based on the specific surface area (square meters per gram) of fly ash. If the specific surface area is proportional to the surface area:volume ratio and if particle sphericity is assumed, then elemental concentration is inversely proportional to particle size. Based on mass transfer arguments, Flagan and and Friedlander (1976) indicated that concentration should be inversely dependent on particle size for Knudsen numbers >1 (i.e., for condensation when the particle size is greater than the mean free path of the depositing gas) and inversely dependent on the square of the particle size for Knudsen numbers <1. Application of this model fits existing data equally as well as the model of Davison et al. (1974). Smith et al. (1978) extended the Flagan and Friedlander (1976) and the Davison et al. (1974) models to include fine particles in which the thickness of the deposited surface layer approached the diameter of the total particle. This modification resulted in concentrations that asymptotically approached maxima at particle size <1 μm. The models were demonstrated to fit the concentration dependence on particle size of reaerosolized, ESP-collected

fly ash. Biermann and Ondov (1978) have proposed a model with an inverse square dependence and an asymptotic maximum for concentration as a function of surface thickness. Their results indicated that the thickness of surface-deposited chemicals is inversely proportional to particle size and that total elemental composition is proportional to $1/d^2$, where l is the thickness of the surface layer and d the diameter of the particle. Analysis of 12-stage impactor data with increased resolution in the submicron region supported the mathematical model. Further studies are required, however, to extend the presently available data on concentration as a function of particle size thus allowing evaluation of the validity of the existing mathematical models.

D. Summary

In summary, most studies of the size dependence of elemental concentrations in coal fly ash support the hypothesis of Natusch et al. (1974); the more volatile elements (or chemical forms) are preferentially associated with fine particles. The fine particle mode (<1.0 μm) in the bimodal elemental distributions is generally considered to be because of coagulation of primary particles (Whitby, 1977). Bimodal size distributions may also result from the presence of multiple mineral forms, some of which may decompose or may be associated with a fine mineral grain size. It should be noted, however, that the bimodal distribution of the very volatile elements (Se, Br, and I) observed in impactor samples may be artifacts due to vapor condensation on the larger particles collected on the first impactor stages. Also, the bimodal distribution of metallurgical elements may be associated with entrainment of corrosion products in the flue gases. Similarly, small particle enhancement of relatively nonvolatile elements may be because of a combination of decomposition, chemical reaction, mineral grain size, or elemental association in the organic phase of coal.

V. MATRIX AND SURFACE COMPOSITION OF COAL FLY ASH

A. Matrix Composition

Elemental analyses of coal fly ash show that the major matrix elements are Al, Si, and Fe together with a few percent of Ca, K, Na, and Ti. Fly ashes derived from western United States sub-bituminous coals generally contain higher levels of calcium than do bituminous coals and lignites.

The actual compounds that constitute the fly ash matrix have been identified only for a comparatively small fraction of the mass. The techniques that have proved most useful for this purpose are x-ray powder diffraction and infrared spectroscopy (Natusch et al., 1975). In addition, selected area electron diffraction has been employed in the identification of small crystals often found associated with the surface of fly ash.

X-Ray powder diffraction studies have demonstrated the presence of α-quartz (SiO_2), mullite ($3Al_2O_3 \cdot 2SiO_2$), hematite (Fe_2O_3), magnetite (Fe_3O_4), lime (CaO), and gypsum ($CaSO_4 \cdot 2H_2O$) in aged fly ash (Natusch et al., 1975; Miguel, 1976). However, there is evidence to suggest that crystalline species, associated with aged fly ash may differ from those in the freshly collected material (Fisher et al., 1976, 1978) because of

either the presence or lack of moisture in storage atmospheres. In addition to these crystalline species, x-ray powder diffraction patterns indicate the presence of a substantial amount of material that is amorphous to x-rays (Fig. 11). The composition of this material has not been established with certainty; however, it is widely accepted that it consists of an impure aluminosilicate glass and constitutes the bulk of the fly ash matrix (Natusch et al., 1975; Walt and Thorne, 1965; Simons and Jeffery, 1960).

Infrared spectroscopic identification of inorganic compounds present in coal fly ash has largely been restricted to the tentative identification of residues of evaporated aqueous leachates (Jakobsen et al., 1978). Several sulfate species have been identified; however, it is not clear whether these represent the actual compounds that existed prior to removal from the fly ash. In addition, studies have been made of glass melts derived from oxides of aluminum, iron, and silicon (Henry et al., 1978). These have provided information that supports the contention that the matrix of coal fly ash is predominantly an aluminosilicate glass.

B. Trace Elemental Distribution

Further insights into the factors that determine the distribution of elements in a bulk fly ash sample have been obtained from multielemental analyses of the 32 subsamples presented in Table IV. Specific concentrations of the elements Al, As, Ba, Ca, Co, Cr, Cs, Dy, Eu, Fe, Ga, Hf, K, La, Mg, Mn, Na, S, Sb, Sc, Si, Sm, Sr, Ta, Ti, Th, Y, and Zn were determined. In addition, x-ray powder diffraction patterns and BET surface areas (by nitrogen adsorption) were obtained (Natusch et al., 1975).

As an aid to the interpretation of the extensive data sets obtained, multivariate statistical analyses, in the form of both common-factor analysis and hierarchical aggregative cluster analysis (Harmon, 1967; Blackith and Reyment, 1971) were employed. Common factor analysis makes it possible to determine the way in which each measured variable in the system is related to a set of n factors common to the system as a whole. The important causalities that give rise to the observed data can thus be inferred. By comparison, cluster analysis permits an objective assessment of the similarity between individual subsamples.

The results obtained indicated that the distributional pattern of trace elements in fly ash is controlled by five major factors. These factors have been interpreted to include particle size, particle composition, and the geochemical behavior of the elements.

Thus, specific distributional patterns are observed for the chalcophile, lithophile, and siderophile elements as classified by Goldschmidt's Geochemical Series (Bertine and Goldberg, 1971; Coles et al., 1979b). It would appear, therefore, that the size factor arises as a result of the volatilization and condensation of certain trace metals as described earlier (Davison et al., 1974). The dependence on particle composition possibly reflects the association of some elements (e.g., As and Mn) with certain types of mineral inclusions. The dependence on geochemical class of the elements, in all probability, reflects the different chemical characteristics of each of these classes under high temperature combustion conditions.

SEM-x-ray analysis has provided further insight into the complexity of the matrix composition of coal fly ash. Elemental analysis of morphologically similar fly ash particles from the NBS fly ash reference material indicated extreme matrix heterogeneity (Pawley and Fisher, 1977). Particles rich in K, Ti, Fe, S, or Ca were observed. Indeed nearly all of the Ti in a field of 100 particles could be accounted for by a single Ti-rich particle. It is interesting to note the extreme matrix heterogeneity of individual particles in the NBS fly ash, a material that is well documented as being homogeneous by macroscopic analytical techniques.

C. Surface Composition

As pointed out in previous sections, the inverse dependence of trace elemental concentration on fly ash particle size is generally held to be due to condensation of metallic species onto particle surfaces from the vapor phase (Davison et al., 1974). One would expect, therefore, to find certain volacilizable elements preferentially concentrated on particle surfaces. This has been observed (Linton et al., 1976, 1977; Keyser et al., 1978).

The techniques that have been employed, to date, in analyzing the surface regions of coal fly ash are electron spectrometry for chemical analysis (ESCA), Auger electron spectrometry (AES), and secondary ion mass spectrometry (SIMS). In addition, some surface analytical information is available using electron microprobe x-ray spectrometry. The operational characteristics of these techniques are summarized briefly as follows (Czandérna, 1975; Kane and Larrabee, 1974; Keyser et al., 1978).

The electron microscope (EM) and microprobe (EP) bombard the sample with a focused beam of electrons to stimulate emission of x-rays characteristic of the elements present. The technique is useful for analyses of individual micrometer-size particles and has a lateral and depth resolution of about 1 μm, determined by the x-ray emission volume. The electron probe microanalyzer is described in Chapter 48.

Surface analysis capabilities of EM and EP are poor since the depth resolution is very much greater than the thickness of the surface layer normally of interest. Indeed, information about elemental surface predominance can be obtained only by varying the energy of the electron beam (depth penetration) or by ion etching of the outer surface and by comparing elemental ratios for inner and outer surfaces.

The ESCA technique employs an x-ray source to eject core-level electrons from the sample. Energy analysis of the resulting photoelectrons provides chemical bonding information since the bonding energies of the core electron are sympathetic to changes in the electronic structure of the valence level. Elements present at levels greater than 1 at. % in the uppermost 20 Å are detected. Depth profiling is achieved by etching the surface with an ion beam between analyses. For details on ESCA (or XPS) see Volume I, Chapter 11.

The utility of ESCA for individual particle analysis is limited because of the difficulty of focusing x-rays to a beam diameter smaller than 1 mm, although recent advances indicate that lateral resolutions of 10 μm are feasible. Normally, the sensitivity of ESCA is insufficient to enable observation of trace constituents unless considerable surface enrichment is encountered.

In AES the emission of Auger electrons is stimulated by bombarding the sample with a beam of electrons. The energy of the secondary Auger electrons is characteristic of the emitting element. Spectra are recorded in the first derivative mode to discriminate against a background of inelastically scattered electrons. Elemental detection limits lie in the range 0.1-1.0 at. % within the analytical volume (depth ~20 Å). Depth profiling is achieved by etching the sample surface with an ion beam (normally Ar^+) as in ESCA. Most AES spectrometers possess microprobe capabilities with incident beam diameters of 1-5 μm.

In SIMS the sample is bombarded with a stream of ions (most commonly, negative oxygen ions) and surface material is physically removed. About 1-10% of the sputtered material is in the form of secondary ions that are mass analyzed by a conventional mass spectrometer.

The ion microprobe represents a special configuration of SIMS in which the primary ion beam can be focused to a diameter of about 3-5 μm. Both individual particle analysis and elemental-mapping capabilities are thus available. Depth profiling constitutes an integral part of the process of secondary ion generation.

A major advantage of SIMS is its extremely high sensivitiy, with elemental detection limits ranging from 10^{-2} - 10^{-6} at. %, depending on the element and the primary ion used. Typically, it is possible to observe as little as 1 μg/g in the analytical volume, thereby enabling studies of species present at trace levels. Secondary ion mass spectrometry is, however, subject to several types of interferences and artifacts. In particular, spectral interferences from molecular- and multiple-charged ions make the high resolving power of a double-focusing mass spectrometer desirable. Also, volatilization losses and migration of sample ions under the influence of the primary ion beam can give rise to spurious depth profiles. Such effects are often difficult to identify in SIMS since removal of surface material is an integral part of the detection process.

Of the above techniques, AES and SIMS are generally most useful for surface analysis and the depth-profiling studies, owing to their sensitivity and good lateral and depth resolution. Electron spectrometry for chemical analysis, however, has the important advantage of providing information about the identity of molecular species present. With all the techniques, difficulties are encountered in establishing even semiquantitative depth scales, which are normally attempted by calibrating the rate of removal of surface material against that obtained for a standard having a surface layer of known thickness. The main problem, however, lies in matching the matrix composition of the standard to that of the material being studied, which, in the case of coal fly ash, is not well defined.

Surface analysis and depth profiling studies of both individual coal fly ash particles and groups of particles have established that a number of trace elements, including C, Cr, K, Mn, Na, Pb, S, Tl, V, and Zn, are substantially surface enriched, whereas the matrix and minor elements, Al, Ca, Fe, Mg, Si, and Ti, are not (Linton et al., 1977). This observation clearly supports the hypothesis that the more volatile elements, or their compounds, are vaporized during combustion and then condense on the surfaces of coentrained fly ash particles at lower temperature.

Depth profiling studies of fly ash have also demonstrated the utility of using instrumental techniques in conjunction with solvent leaching to remove soluble surface material. An example of this approach is presented in Fig. 12 for the elements Pb and Tl. This study demonstrated that extraction of fly ash with water or dimethyl sulfoxide removes the surface layer of both elements. Determination of the amounts of Pb and Tl in solution then enables estimation of the amounts present in the surface layer. Assuming a surface layer thickness of 300 Å, one obtains average concentrations of 2700 ug/g for Pb and 920 ug/g for Tl in the surface layer as compared to bulk particulate concentrations of 620 ug/g and 30 ug/g for these elements. Similar estimates for several other trace elements are presented in Table VII (Natusch, 1978a).

Solvent leaching can also provide some insight into the chemical forms of elements present. For example, although AES and SIMS indicate little surface enrichment of iron, aqueous leaching rapidly removes this element from the surface region, thereby indicating its presence in a readily soluble form. Similarly, comparison of the leaching and depth profiles of K, Fe, Na, and S suggests that these elements may be associated with each other in the surface layer, possibly as alkali-iron sulfates. Further support of the existence of simple and/or complex sulfates is provided by ESCA studies that show that the oxidation states of Fe and S in the surface region are +3 and +6, respectively (Wallace, 1974).

Surface analytical results, such as those presented in Fig. 12 and Table VII demonstrate the considerable differences in composition that exist between the interior of fly ash particles and their external surface. Since it is the particle surface that is in contact with the external environment, determination of surface composition is of considerable importance, as previously discussed. Finally, it should be remarked that there are no coherent data that relate surface composition to particle size for fly ash. However, if the volatilization-condensation process is primarily responsible for surface enrichment of trace elements, then one would not expect surface concentrations to vary greatly with particle size. This is because the amount of vapor deposited is proportional to surface area, thereby resulting in a constant elemental concentration per unit surface area. Of course, if other mechanisms are responsible for or contribute to surface enrichment (e.g., agglomeration of accumulation mode particles with coarse particles or thermal diffusion of trace species to the surface of molten particles), then some dependence on particle size would be anticipated.

D. Solubility and Leachability

A number of workers (Shannon and Fine, 1974; Theis and Wirth, 1977; James et al., 1977; Dreesen et al., 1977) have reported that the bulk solubility of coal fly ash in water is very low and rarely exceeds 2-3% by weight. The bulk solubility is clearly a property of both the glassy and crystalline matrix materials identified earlier, and one would expect elements that are either chemically or physically trapped within this matrix to exhibit low solubility. On the other hand, at least some of the material present in the surface skin is readily soluble in water (Fig. 12). Indeed, it is now quite well established (Linton et al., 1977; Natusch, 1978a; Fisher et al., 1978e) that most of the soluble fraction of fly ash is derived from this surface layer and is thus very rich in trace elements.

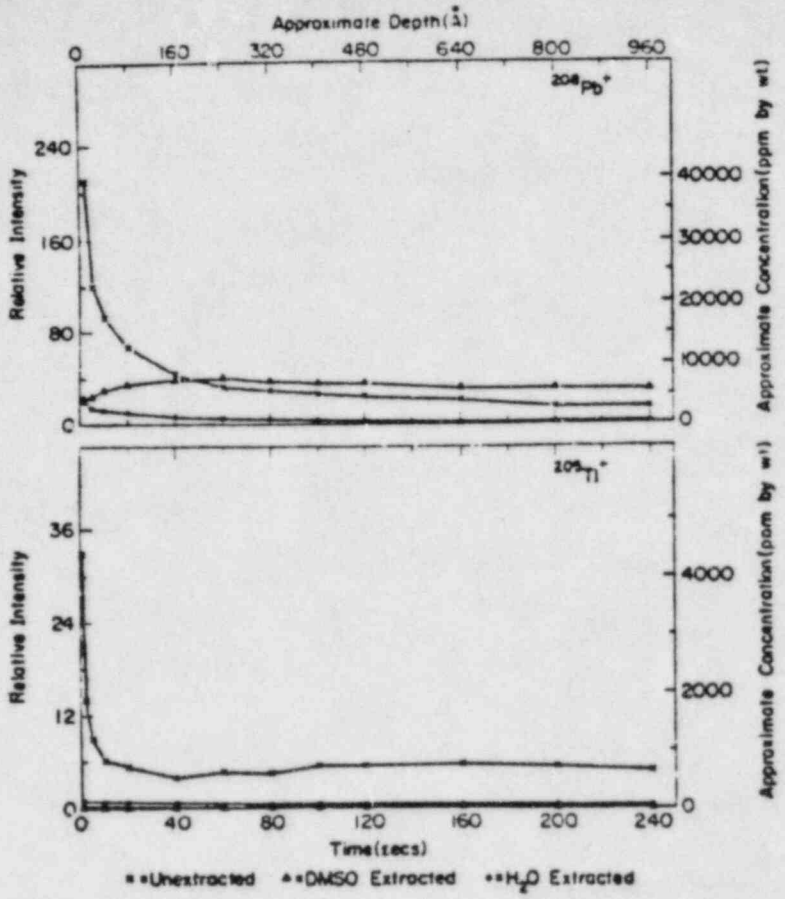

Fig. 12. Ion microprobe depth profiles for Pb and Tl for unextracted and extracted fly ash samples (reprinted with permission from R. W. Linton, P. Williams, C. A. Evans, Jr. and D. F. S. Natusch, Anal. Chem. 49, 1514 (1977). Copyright 1977 by the American Chemical Society).

Table VII. Estimated Surface Concentrations of Elements in Coal Fly Ash[a]

Element	Bulk concentration (μg/g)	Estimated surface concentration in 300 Å layer (μg/g)
As	600	1500
Cd	24	700
Co	65	440
Cr	400	1400
Pb	620	2700
S	7100	252,000
V	380	760

[a] From Natusch (1978a).

At the present time, there is considerable confusion involved in interpreting and understanding results obtained from different studies of fly ash solubility. Specifically, quite different results are obtained by workers using apparently similar laboratory leaching techniques and none are readily transferrable to field studies. It is appropriate, therefore, to consider the factors that control leachate composition under both laboratory and field conditions and to standardize one or more laboratory leaching techniques whose results bear some relationship to real field conditions.

Some insight into leaching behavior can be obtained by recognizing that soluble inorganic species M_iA_i associated with fly ash particles can dissociate into their component cations M_i and anions A_i in aqueous solution, and that both dissolution and deposition (e.g., precipitation) processes can occur. Furthermore, cations and anions present in solution can interact so as to set up multiple equilibria that may involve ion pairing, complexation, precipitation, or acid-base behavior (M_iA_j or M_jA_i). The result can be expressed, simplistically by the equations

$$P \sum_i^n M_iA_i \underset{k_{-1}}{\overset{k_1}{\rightleftharpoons}} P + \sum_i^n M_i + \sum_i^n A_i + \sum_j^m A_j + \sum_j^m M_j \qquad (10)$$

$$k_{-2}+k_2 \qquad k_{-3}+k_3$$

$$\sum_{ij}^{mn} M_iA_j \qquad \sum_{ij}^{mn} M_jA_i$$

Here P represents the parent particles and k_n, k_{-n} are the rate constants for forward and reverse reactions, respectively. It is apparent from Eq. (10) that, when leaching studies are conducted under batch conditions, such that the amount of fly ash and solvent are maintained constant, an equilibrium will be established between particulate and solution species. Consequently, only a fraction of the potentially soluble material will enter solution. On the other hand, if conditions are such that soluble material is continuously removed by provision of fresh solvent or by providing a large solution sink in the form of complexing ligands or acids, then all potentially soluble material will ultimately enter solution.

Matusiewicz and Matusch (1979) have conducted very extensive studies to demonstrate the validity of Eq. (10). They have established that the rate and extent of leaching depend upon the leaching method, the fly ash:solution ratio, temperature, pH, complexing agents, particle size, and fly ash origin exactly as predicted from Eq. (10) for both equilibrium and nonequilibrium conditions. When equilibrium is established between particulate and solution species, as in batch leaching, little dependence on particle

size is observed since the amount of a given element is determined by its solution concentration (solubility) that is only weakly related to the amount of solid phase present. Exhaustive (nonequilibrium) leaching, however, removes all soluble material, the amount of which is directly related to particle size because of its presence in fly ash surface layer.

It is apparent from the foregoing remarks that any leaching process that establishes the solid-solution equilibrium given in Eq. (10) will result in changes in solution composition with equilibrium position. It is hardly surprising, therefore, that widely differing results are obtained by workers who use different leaching conditions. Nevertheless, some significant generalizations can be made. First, it is readily apparent that much higher proportions of most trace elements are soluble than is the case for matrix elements (Table VIII). This is due, in part, to the predominance of trace elements in the particle surface layers in quite soluble forms (probably sulfates, oxides, and carbonates). Second, it is clear that, under batch leaching conditions, such as are most likely to occur in the field, the amount of each element entering solution is strongly dependent on the dilution (fly ash:water ratio) and the initial pH (Matusiewicz and Natusch, 1979; Dreesen et al., 1977; Theis and Wirth, 1977).

Table VIII. Percentage of Elements Leached from a Typical Coal Fly Ash[a]

Element	% Leached
Al	0.2
B	5
Ba	4
Ca	35
Cr	30
K	40
Mg	0.2
Mn	0.4
Mo	85
Na	10
P	6
Pb	100
Si	0.1
Sr	6
Zn	6

[a] From Matusiewicz and Natusch (1979).

E. Organic Constituents

To date, no exhaustive determination of organic species associated with coal fly ash has been reported. Rather, emphasis has been placed primarily on the determination of polycyclic organic matter (POM) in fly ash, due to the potential carcinogenicity of several compounds of this type (Committee of Biological Effects of Atmospheric Pollutants, 1972). For the most part, the several studies of POM in fly ash have indicated either extremely low or undetectable levels (Committee on Biological Effects of Atmospheric Pollutants, 1972).

In a survey of fly ashes representing several coals and combustion conditions, Aslund et al., (1978) found no individual species of POM to be present at concentrations greater than 20 ng/g. A number of other unidentified organic compounds were, however, observed at somewhat higher (10x) concentrations. It is important to note that all of these studies have considered fly ash collected in bulk from power plant control devices.

Only a few studies have been made of POM present in fly ash that was actually emitted and collected from the atmosphere (Natusch, 1978b; Tomkins, 1978; Stahley, 1976). However, all have indicated concentrations that are very much greater than encountered in fly ash collected within the plant. This apparent paradox has been explained by Natusch and Tomkins (1977) who postulate that POM (and probably other organic species) are present as gases at the temperatures encountered within a power plant but rapidly and quantitatively adsorb onto surfaces of emitted fly ash particles as the temperature falls on leaving the stack. Both laboratory (Miguel et al., 1979) and field (Miguel, 1976; Natusch, 1978b) studies support this hypothesis.

The actual compounds that have been identified in emitted fly ash are listed in Tables IX and X, which present the results of two separate studies in which specific concentrations inside and outside the plant, and volume concentrations in the plume, were determined. To our knowledge, only one study has actually measured POM concentrations as a function of particle size for emitted fly ash (Natusch, 1978b). The results indicated little convincing dependence of concentration on aerodynamic particle size over the range <1.1 to >7.0 μm. However, the fly ash in question was derived from a small plant that employed a chain grate stoker, and the particles were found to be extremely irregular in outline. Furthermore, there was very little change in specific surface area over the size range collected. We do not, therefore, consider these results to be conclusive.

In fact, if the temperature dependent adsorption mechanism proposed by Natusch and Tomkins (1977) is correct, one would expect the specific concentration of organic species to vary in proportion to the surface area of the fly ash particles. There is some indirect evidence for this behavior (Chrisp et al., 1978; Fisher et al., 1979c), but further work is clearly required. It has been established, however, that adsorption of POM (pyrene) onto fly ash under laboratory conditions occurs, to significantly different extents, on different fly ashes and on magnetic and nonmagnetic fractions of a given fly ash (Miguel, 1976; Korfmacher et al., 1979a).

Table IX. Measurement of Polycyclic Organic Matter Emitted from a Coal-Fired Power Plant Stack[a]

Compound	Specific concentration (ug/g)	
	Inside stack	Outside stack
Fluorene	ND[b]	Trace
Phenanthrene	ND	9
Fluroanthene	ND	19
Pyrene	ND	12
Benzofluorene	ND	2
1-methylpyrene	ND	1
Benzophenanthrene	ND	3
Benzo[a]pyrene	ND	5
Total fluorescence	3.61×10^{-3} units	3.68 units

[a] From Tomkins (1978).

[b] Not detectable.

Table X. Emission Factors for Polycyclic Organic Matter from Coal Fired Furnaces in (pounds/ton of coal) x 10^4 [a]

Species	Pulverized firing	Chain grate stoker	Hand fired
Benzo[a]pyrene	0.2-0.52	0.3	3520
Pyrene	0.8-1.6	3.5	5260
Benzo[e]pyrene	0 -2.3	1.1	880
Perylene	0 -0.6	--	526
Fluoranthene	--	6.0	8800

[a] Committee on Biological Effects of Atmospheric Pollutants, 1972.

Finally, it should be mentioned that POM associated with fly ash may undergo chemical transformation following adsorption and emission. In this regard, Korfmacher et al., (1979b) have shown that adsorption onto coal fly ash effectively stabilized most POM against photochemical decomposition, but actually promotes rapid (hours to days) non-photochemical oxidation of polycyclic aromatic compounds possessing one benzylic carbon atom. Furthermore, Hughes and Natusch (1978) have shown that exposure of POM adsorbed on fly ash to typical plume concentrations of sulfur dioxide and nitrogen oxides results in very rapid formation of a variety of derivatives having sulfur or nitrogen containing substituents. It is possible, therefore, that the chemical nature of POM associated with coal fly ash emitted from a power plant is likely to change dramatically with time and distance from the plant.

REFERENCES

Andren, A. W., and Klein, D. H. (1975). Environ. Sci. Technol. 9, 856-858.

Aslund, A., Miller, M., Natusch, D. F. S., and Taylor, D. R. (1978). Unpublished results.

Bertine, K. K., and Goldberg, E. D. (1971). Science 173, 233-235.

Bickelhaupt, R. E. (1974). J. Air Pollut. Control Assoc. 24, 251-255.

Bickelhaupt, R. E. (1975). J. Air Pollut. Control Assoc. 25, 148-152.

Biermann, A. H., and Ondov, J. M. (1978). "Application of Surface-Deposition Models to Size-Fractionated Coal Fly Ash," Prepr. UCRL-81361. Lawrence Livermore Lab., Livermore, California.

Billings, C. E., and Matson, W. R. (1972). Science 176, 1232-1233.

Billings, C. E., Sacco, A. M., Matson, W. R., Griffin, R. M., Coniglio, W. R., and Harley, R. A. (1973). J. Air Pollut. Control Assoc. 23, 773-777.

Blackith, R. E., and Reyment, R. A. (1971). "Multivariate Morphometrics." Academic Press, New York.

Butcher, S. S., and Charlson, R. J. (1972). "An Introduction to Air Chemistry." Academic Press, New York.

Campbell, J. A., Laul, J. C., Nielson, K. K., and Smith, R. D. (1978). Anal. Chem. 50, 1032-1040.

Carter, J. L., and MacGregor, I. D. (1970). Science 167, 661-663.

Cheng, R. J., Mohnen, V. A., Shen, T. T., Current, M., and Hudson, J. B. (1976). J. Air Pollut. Control Assoc. 26, 727-824.

Chrisp, C. E., Fisher, G. L., and Lammert, J. E. (1978). Science 199, 73-74.

Coles, D. G., Ragaini, R. C., and Ondov, J. M. (1978). Environ. Sci. Technol. 12, 442-446.

Coles, D. G., Ragaini, R. C., Ondov, J. M., Fisher, G. L., Silberman, D., and Prentice, B. A. (1979). Environ. Sci. Technol. 13, 455-459.

Committee on Biological Effects of Atmospheric Pollutants (1972). "Particulate Polycyclic Organic Matter." Natl. Acad. Sci., Washington, D. C.

Czanderna, A. W., ed. (1975). "Methods of Surface Analysis," Elsevier, Amsterdam.

Davison, R. L., Natusch, D. F. S., Wallace, J. R., and Evans, C. A., Jr. (1974). Environ. Sci. Technol. 8, 1107-1113.

Diehl, R. C., Hattman, E. A., Schultz, H., and Haren, R. J. (1972). "Fate of Trace Mercury in the Combustion of Coal." Tech. Prog. Rep. No. 54. Bur. Mines, Managing Coal Wastes Pollut. Program, Pittsburgh Energy Res. Cent., Pittsburgh, Pennsylvania.

Dreesen, D. R., Gladney, E. S., Owens, J. W., Perkins, B. L., Wienke, C. L., and Wangen, L. E. (1977). Environ. Sci. Technol. 11, 1017-1019.

Fisher, G. L., and Chrisp, C. E. (1978). Symp. Appl. Short-Term Bioassays Fractionation Anal. Complex Environ. Mixtures. (Waters, M. D., Nesnow, S., Haisiagh, J. L., Sandhu, S. S., and Claxton, L., eds.) EPA 60019-78-027, pp. 441-462, Williamsburg, Va.

Fisher, G. L., and Natusch, D. F. S. (1979). U. S. Dept. Energy, NTIS UCD-472-502.

Fisher, G. L., Chang, D. P. Y., and Brummer, M. (1976). Science 192, 553-555.

Fisher, G. L., Prentice, B. A., Silberman, D., Ondov, J. M., Ragaini, R. C., Biermann, A. H., McFarland, A. R., and Pawley, J. B. (1977). Jt. Chem. Inst. Can./Am. Chem. Soc. Meet., 2nd Div. Fuel Chem. Symp., Properties Coal Ash, Montreal.

Fisher, G. L., Prentice, B. A., Silberman, D., Ondov, J. M., Ragaini, R. C., Biermann, A. H., and McFarland, A. R. (1978c). Environ, Sci. Technol. 12, 447-451.

Fisher, G. L., Chrisp, C. E., and Hayes, T. L. (1979a). Conf. Carbonaceous Part. Atmos., Berkeley, Calif. in press.

Fisher, G. L., Hayes, T. L., Prentice, B. A., and Lai, C. (1979b). In "Radiobiology Laboratory Annual Report," UCD 472-125, Univ. of California, Davis. in press.

Fisher, G. L., Chrisp, C. E., and Raabe, O. G. (1979c). Science 204, 879-881.

Fisher, G. L., Silberman, D., Prentice, B. A., Heft, R. E., and Ondov, J. M. (1979d). Environ. Sci. Technol. 13, 689-693.

Flagan, R. C., and Friedlander, S. K. (1976). Symp. Aerosol Sci. Technol., Meet. Am. Inst. Chem. Eng., 82nd, Atlantic City, N.J.

Gay, N. C. (1976). Science 194, 724-725.

Gibbon, D. L. (1978). Personal communication, Guilford Coll., Greensboro, North Carolina.

Gladney, E. S., Small, J. A., Gordon, G. E., and Zoller, W. H. (1976). Atmos. Environ. 10, 1071-1077.

Gordon, G. E., and Zoller, W. H. (1973). Proc. Annu. NSF Trace Contaminants Conf., 1st, Oak Ridge Natl. Lab., Oak Ridge, Tenn. CONF-730802, pp. 314-325.

Gordon, G. E., Zoller, W. H., and Gladney, E. S. (1974). In "Trace Substances in Environmental Health - VII. A Symposium" (D. D. Hemphill, ed.), pp. 161-166. Univ. of Missouri, Columbia.

Harmon, H. H. (1967). "Modern Factor Analysis," 2nd Ed. Univ. of Chicago Press, Chicago, Illinois.

Henry, W. M., Mitchel, R. I., and Knapp, K. T. (1978). Proc. Workshop Primary Sulfate Emiss. Combust. Sources, Southern Pines, North Carolina EPA Rep. No. 600/9-78-020b, Vol. II, pp. 185-208.

Hughes, M. M., and Natusch, D. F. S. (1978). Unpublished results.

Jakobsen, R. J., Gendreau, R. M., Henry, W. M., and Knapp, K. T. (1978). Proc. Workshop Primary Sulfate Emiss. Combust. Sources, Southern Pines, North Carolina EPA Rep. No. 600/9-78-020b, Vol. I, pp. 253-274.

James, W. D., Janghorbani, M., and Baxter, T. (1977). Anal. Chem. 49, 1994-1997.

Kaakinen, J. W., Jorden, R. M., Lawasani, M. H., and West, R. E. (1975). Environ. Sci. Technol. 9, 862-69.

Kalb, W. G. (1975). In "Trace Elements in Fuel" (S. P. Babu, ed.), Advances in Chemistry Series, No. 141, pp. 154-174. Am. Chem. Soc., Washington, D. C.

Kane, P. F., and Larrabee, G. B., eds. (1974). "Characterization of Solid Surfaces." Plenum, New York.

Newton, G. J., Raabe, O. G., and Mokler, B. V. (1977). J. Aerosol. Sci. 8, 339-347.

Olsen, K. W., and Skogerboe, R. K. (1975). Environ. Sci. Technol. 9, 227-230.

Ondov, J. M., Ragaini, R. C., and Biermann, A. H. (1976). Prepr. Pap. Natl. Meet. Div. Environ. Chem., Am. Chem. Soc., San Francisco, Calif. 200-203.

Ondov, J. M., Ragaini, R. C., Heft, R. E., Fisher, G. L., Silberman, D., and Prentice, B. A. (1977a). Mater. Res. Symp., 8th, Natl. Bur. Stand., Gaithersburg, Md. pp. 565-572.

Ondov, J. M., Ragaini, R. C., Biermann, A. H., Choquette, C. E., Gordon, G. E., and Zoller, W. H. (1977b). Prepr. Pap. Natl. Meet., Div, Environ, Chem., Am. Chem. Soc., New Orleans, La.

Ondov, J. M., Ragaini, R. C., and Biermann, A. H. (1977c). "Elemental Emissions and Particle-Size Distributions of Minor and Trace Emissions at Two Western Coal-Fired Power Plants Equipped with Cold-Side Electrostatic Precipitators." Prepr. UCRL-80254. Lawrence Livermore Lab., Livermore, California.

Ondov, J. M., Ragaini, R. C., and Biermann, A. H. (1979). Environ. Sci. Technol. 13, 598-607.

Padia, A. S., Sarofim, A. F., and Howard, J. B. (1976). Combust. Inst. Cent. States Sect. Spring Meet., Columbus, Ohio.

Parks, N. J., Raabe, O. G., Bradley, E. W., Teague, S., and Hopkins, B. (1977). In "Radiobiology Laboratory Annual Report," pp. 77-82. Univ. of California, Davis.

Pawley, J. B., and Fisher, G. L. (1977). J. Microsc. (Oxford) 110, 87-101.

Raabe, O. G. (1976). APCA J. 26, 856-860.

Raabe, O. G. (1978). Environ. Sci. Technol. 12, 1162-1167.

Raask, E. (1966). ASME Trans. J. Eng. Power 88, 40-44.

Raask, E. (1968). J. Inst. Fuel 43, 339-344.

Ragaini, R. C., and Ondov, J. M. (1977). J. Radioanal. Chem. 37, 679-691.

Ruch, R. R., Gluskoter, H. J., and Shimp, J. F. (1974). Ill. State Geol. Surv., Rep. No. 72.

Sarofim, A. F., Howard, J. B., and Padia, A. S. (1977). Combust. Sci. Technol. 16, 187-204.

Shannon, D. G., and Fine, L. O. (1974). Environ. Sci. Technol. 8, 1026-1028.

Simons, H. S., and Jeffery, J. W. (1960). J. Appl. Chem. 10, 328-336.

Small, J. A. (1976). Ph.D. Thesis, Univ. of Maryland, College Park.

Smith, R. D., Campbell, J. A., and Nielson, K. K. (1979). Environ. Sci. Technol. 13, 553-558.

Southern Research Institute (1975). "Survey of Information on Fine Particle Control," Rep. No. 259, Electr. Power Res. Inst., Palo Alto, California.

Stahley, S. (1976). Personal communication.

Task Group on Lung Dynamics. (1966). Health Phys. 12, 173-207.

Theis, T. L., and Wirth, J. L. (1977). Environ. Sci. Technol. 11, 1096-1100.

Tomkins, B. A. (1978). Ph.D. Thesis, Univ. of Illinois, Urbana.

Vandegraft, A. E., Shannon, L. J., and Gorman, P. G. (1973). Chem. Eng. 80, 107-114.

Waits, G. A., McKay, D. S., and Gibbon, D. L. (1978). Personal communication, SN6, NASA-JSC, Houston, Texas.

Wallace, J. R. (1974). Ph.D. Thesis, Univ. of Illinois, Urbana.

Wait, J. D., and Thorne, D. J. (1965). J. Appl. Chem. 15, 585-604.

Wangen, L. E., and Wienke, C. L. (1976). "A Review of Trace Element Studies Related to Coal Combustion in the Four Corners Area of New Mexico," Informal Rep. LA-6401-MS. Los Alamos Sci. Lab., Los Alamos, New Mexico.

Whitby, K. T. (1977). Mater. Res. Symp., 8th, Natl. Bur. Stand., Gaitherburg, Md. pp. 165-173.

White, H. J. (1963). "Industrial Electrostatic Precipitation," Addison-Wesley, Reading, Massachusetts.

Yeh, H. C., Phalen, R. F., and Raabe, O. G. (1976). Environ. Health Perspect. 15, 147-156.

Zoller, W. H., Gladney, E. S., Gordon, G. E., and Bors, J. J. (1974). In "Trace Substances in Environmental Health - VIII. A Symposium" (D. D. Hemphill, ed.), pp. 167-172. Univ. of Missouri, Columbia.